

Multiuser-MIMO Systems Using Comparator Network-Aided Receivers With 1-Bit Quantization

Ana Beatriz L. B. Fernandes, Zhichao Shao, *Member, IEEE*,

Lukas T. N. Landau, *Senior Member, IEEE* and Rodrigo C. de Lamare, *Senior Member, IEEE*

Abstract

Low-resolution analog-to-digital converters (ADCs) are promising for reducing energy consumption and costs of multiuser multiple-input multiple-output (MIMO) systems with many antennas. We propose low-resolution multiuser MIMO receivers where the signals are simultaneously processed by 1-bit ADCs and a comparator network, which can be interpreted as additional virtual channels with binary outputs. We distinguish the proposed comparator networks in fully and partially connected. For such receivers, we develop the low-resolution aware linear minimum mean-squared error (LRA-LMMSE) channel estimator and detector according to the Bussgang theorem. We also develop a robust detector which takes into account the channel state information (CSI) mismatch statistics. By exploiting knowledge of the channel coefficients we devise a mean-square error (MSE) greedy search and a sequential signal-to-interference-plus-noise ratio (SINR) search for optimization of partially connected networks. Numerical results show that a system with extra virtual channels can outperform a system with additional receive antennas, in terms of bit error rate (BER). Furthermore, by employing the proposed channel estimation with its error statistics, we construct a lower bound on the ergodic sum rate for a linear receiver. Simulation results

A. B. L. B. Fernandes, L. T. N. Landau and R. C. de Lamare are with the Centro de Estudos em Telecomunicações, Pontifícia Universidade Católica do Rio de Janeiro, Rio de Janeiro CEP 22453-900, Brazil, (e-mail: anafernandes@cetuc.puc-rio.br; lukas.landau@cetuc.puc-rio.br; delamare@cetuc.puc-rio.br). Z. Shao is with the National Key Laboratory of Science and Technology on Communications, University of Electronic Science and Technology of China, Chengdu 611731, China (e-mail: zhichao.shao@uestc.edu.cn). Parts of this work, have been presented on the 2020 54th Asilomar Conference on Signals, Systems, and Computers [1] and on the IEEE Statistical Signal Processing Workshop 2021 (SSP) [2]. This work is based on the thesis [3] of A. B. L. B. Fernandes. This work has been supported by the ELIOT ANR18-CE40-0030 and FAPESP 2018/12579-7 project and FAPERJ.

confirm that the proposed approach outperforms the conventional 1-bit MIMO system in terms of BER, MSE and sum rate.

Index Terms

Multiuser MIMO, 1-bit ADCs, Comparator Network, Channel Estimation, Signal Detection

I. INTRODUCTION

Large-scale Multiple-Input Multiple-Output (MIMO) technology is a promising approach for future wireless communication networks that scale up in speed and bandwidth. There are many advantages compared to current systems including high spectral efficiency and less propagation loss caused by channel fading, among others [4]. However, there are still some practical challenges when it comes to the deployment of a large number of antennas at the base station (BS), such as the hardware cost and power consumption. For instance, the power consumption of ADCs scales exponentially with the number of quantization bits [5]. Therefore, the use of current high-speed and high-resolution ADCs (8-12 bits) for each antenna array would become a great burden to the BS. Consequently, the use of low-cost and low-resolution ADCs (1-3 bits) are promoted as a potential solution to this problem [6]–[8].

A. Motivation and Prior Works

Many works have studied large-scale multiuser MIMO systems with low resolution ADCs at the front-end. Specifically, 1-bit ADCs are of interest in such systems due to their low power consumption. A commonly used technique to mitigate the performance loss caused by the coarse quantization is oversampling, where the received signal is sampled at a rate faster than the Nyquist rate [9]. In this regard, the studies in [10]–[13] have considered temporal oversampling at the receiver in order to achieve better channel estimation and detection performance. However, for temporal oversampling, the computational complexity is relatively high for receive processing.

Channel estimation is another problem that currently limits the performance of coarsely quantized systems. Several papers have investigated channel estimation for quantized massive MIMO systems such as least squares (LS) [14], recursive least squares (RLS) [15], approximate message passing (AMP) [16] and generalized approximate message passing (GAMP) [17]. Another sophisticated channel estimator is given by the near maximum likelihood (nML) estimator devised in [18]. The authors in [19] have developed a Bussgang linear minimum mean squared

error (BLMMSE) channel estimator, where lower bounds on the theoretical achievable rate for maximum ratio combiner (MRC) and zero-forcing (ZF) receivers are derived. The linear Bussgang based channel estimation was generalized for 1-bit ADCs with nonzero thresholds in [20], where the authors also devised the optimization of the thresholds. Moreover, maximum a-posteriori probability (MAP) channel estimators and the corresponding performance analysis have been studied in [21], [22]. The work in [23] develops a channel estimator by taking spatial and temporal correlations into consideration. Furthermore, the low complexity channel estimator and its corresponding achievable rate from [24] rely on a model with infinite number of channel taps, and independent and identically distributed quantization noise.

Several works related to signal detection in systems with low-resolution ADCs are: iterative detection and decoding (IDD) [25], sphere decoding [26] and nML [18]. Moreover, coarse quantization in large-scale MIMO systems has been considered in a number of different aspects and approaches. Recently, the authors in [27], [28] have considered spatial oversampling by employing a 1-bit Sigma-Delta ($\Sigma\Delta$) sampling scheme which has shown large performance gains on channel estimation and signal detection. For the case of receivers with multi-bit ADCs, the design of a proper automatic gain control (AGC) can be relevant in order to minimize the signal distortion due to the coarse quantization [29]. Furthermore, the studies in [30]–[33] have devised different precoding techniques which rely on coarse quantization at the transmitter.

B. Main Contributions

The scope of this study lies in the design of a novel multiuser MIMO receiver architecture that uses 1-bit ADCs. The proposed multiuser MIMO receiver includes a comparator network with binary outputs which can compare signals from different antennas in terms of real and imaginary parts. The additional comparator network can be interpreted as additional virtual channels that aid further receive processing such as detection and channel estimation. As the virtual channels can be seen as an alternative to additional receive antennas the proposed approach is especially promising for receivers with limited number of antennas due to space constraints.

Two types of comparator networks are proposed, i.e., fully and partially connected networks. The design of partially connected networks is a combinatorial problem, which can be computationally very costly. Two suboptimal design methods are proposed in terms of a MSE based Greedy Search-based algorithm and a sequential SINR based search algorithm, which require much less comparators to approach a comparable detection performance as the

performance with fully connected networks. Numerical results confirm that detection and channel estimation performance can be significantly improved when adding a comparator network to the conventional 1-bit multiuser MIMO receiver. Based on the proposed detector, a sum rate analysis is presented. Simulation results show that the proposed comparator network based-systems yield significantly higher sum rate performance in comparison to the conventional 1-bit multiuser MIMO receiver.

The contributions of this work can be summarized as follows:

- Proposal of a novel multiuser MIMO receiver architecture with 1-bit ADCs and partially or fully connected comparator networks.
- Development of the statistically equivalent linear model for the novel receiver with comparator network.
- Development of a linear MSE based channel estimation for the novel receiver with comparator network and calculation of the channel estimation error statistics.
- Development of a linear MSE based detector for the novel receiver and a robust version that takes into account channel estimation error statistics.
- Sum rate analysis in terms of construction of a lower bound.
- A study of cost and power consumption of the proposed architecture.

Note also that contributions of the proposed study go significantly beyond the contributions of the associated conference papers [1], [2] and the thesis [3], in terms of the generalized robust detection method in Section IV-B, a more practical approach for optimization of comparator networks in Section V-D, the study about the power consumption in Section VI-B and simulation results with more realistic scenarios.

C. Organization of the Paper and Notation

The remainder of this paper is organized as follows: Section II describes the general system model, whereas Section III derives the LRA-LMMSE channel estimator for the proposed system. Section IV details the derivation of the LRA-LMMSE detector and a robust version of it, while Section V describes the insight and the design of the comparator network and Section VI shows the complexity analysis of the proposed system. Section VII presents the construction of the lower bound on the sum rate. Then, Section VIII presents and discusses the numerical results. Finally, Section IX gives the conclusions.

Regarding the notation, bold upper and lower case letters such as \mathbf{A} and \mathbf{a} denote matrices and vectors, respectively. \mathbf{I}_n is a $n \times n$ identity matrix. The vector or matrix transpose and conjugate transpose are represented by $(\cdot)^T$ and $(\cdot)^H$. $\Re\{\cdot\}$ and $\Im\{\cdot\}$ get the real and imaginary part from the corresponding vector or matrix, respectively. Additionally, $\text{diag}(\mathbf{A})$ is a diagonal matrix only containing the diagonal elements of \mathbf{A} . The inverse of the sine function is denoted by $\sin^{-1}(\cdot)$. Moreover, $\text{vec}(\mathbf{A})$ is the vectorized form of \mathbf{A} obtained by stacking its columns, while the inverse of this operation is $\text{unvec}(\mathbf{a})$, depending on the context. The expectation operator is denoted as $E[\cdot]$. The Kronecker product is denoted by \otimes .

II. SYSTEM MODEL

The general system model for the proposed comparator network-aided 1-bit multiuser MIMO system is illustrated with a block diagram in Fig. 1, where the received signal \mathbf{y} , of dimensions $(N_r \times 1)$, for the uplink of a single-cell multiuser MIMO system with N_t single-antenna users and N_r receive antennas is written as

$$\mathbf{y} = \mathbf{H}\mathbf{x} + \mathbf{n}. \quad (1)$$

The vector \mathbf{x} contains complex transmit symbols of the N_t users with transmit power $E\{\Re\{x_i\}^2\} = E\{\Im\{x_i\}^2\} = \frac{1}{2}\sigma_x^2$, $\mathbf{H} \in \mathbb{C}^{N_r \times N_t}$ is the channel matrix and $\mathbf{n} \in \mathbb{C}^{N_r \times 1}$ is the noise vector where each element is complex Gaussian distributed with $\mathcal{CN}(0, \sigma_n^2)$.

The real-valued system model can be written as

$$\begin{bmatrix} \Re\{\mathbf{y}\} \\ \Im\{\mathbf{y}\} \end{bmatrix} = \begin{bmatrix} \Re\{\mathbf{H}\} & -\Im\{\mathbf{H}\} \\ \Im\{\mathbf{H}\} & \Re\{\mathbf{H}\} \end{bmatrix} \begin{bmatrix} \Re\{\mathbf{x}\} \\ \Im\{\mathbf{x}\} \end{bmatrix} + \begin{bmatrix} \Re\{\mathbf{n}\} \\ \Im\{\mathbf{n}\} \end{bmatrix}. \quad (2)$$

A more compact notation for (2) reads as

$$\mathbf{y}_R = \mathbf{H}_R \mathbf{x}_R + \mathbf{n}_R, \quad (3)$$

where $\mathbf{y}_R \in \mathbb{R}^{2N_r \times 1}$, $\mathbf{H}_R \in \mathbb{R}^{2N_r \times 2N_t}$ and $\mathbf{x}_R \in \mathbb{R}^{2N_t \times 1}$. The received signal is then forwarded to the 1-bit ADCs and the comparator network (shown in Fig. 2). Each comparator compares two received signals and quantizes the difference as $\{\pm 1\}$. Accordingly, each comparator process can be divided into a subtraction and a quantization step. The subtractions are described by the multiplication of \mathbf{y}_R with the matrix \mathbf{B}' and the quantizations are equivalent to the quantization operations that describe the 1-bit ADCs.

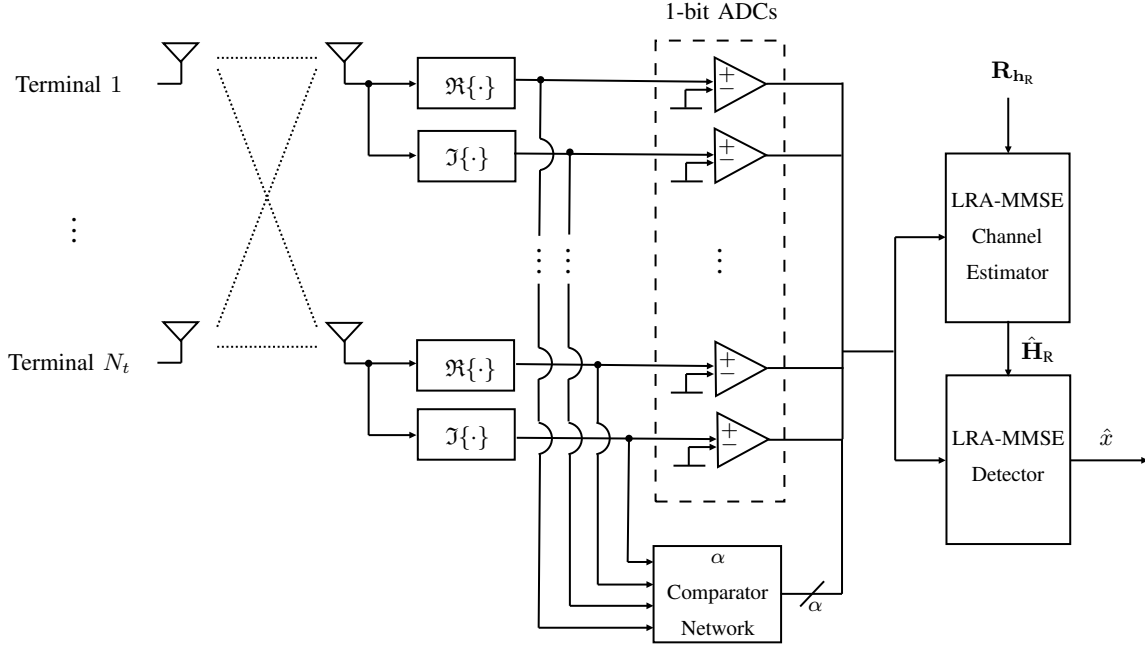


Fig. 1: System model of comparator network based 1-bit MIMO systems.

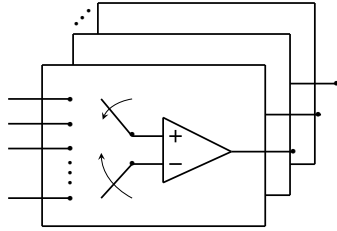


Fig. 2: Schematic of the comparator network.

Letting $Q(\cdot)$ represent the 1-bit quantization, the output of the ADCs and the comparator network is described by

$$\mathbf{z}_Q = Q \left(\begin{bmatrix} \mathbf{y}_R \\ \mathbf{B}' \mathbf{y}_R \end{bmatrix} \right) = Q \left(\begin{bmatrix} \mathbf{I}_{2N_r} \\ \mathbf{B}' \end{bmatrix} \mathbf{y}_R \right), \quad (4)$$

where $\mathbf{B}' \in \mathbb{R}^{\alpha \times 2N_r}$ refers to the comparator network with the form

$$\mathbf{B}' = \begin{bmatrix} \mathbf{B}'_R & \mathbf{B}'_I \end{bmatrix} = \frac{1}{\sqrt{2}} \begin{bmatrix} 1 & -1 & 0 & 0 & \cdots & 0 \\ 0 & 0 & 0 & -1 & \cdots & 1 \\ \vdots & \vdots & \vdots & \vdots & \vdots & \vdots \\ 0 & 1 & 0 & 0 & \cdots & -1 \end{bmatrix}. \quad (5)$$

In each row of \mathbf{B}' , there is only one pair of 1 and -1 and the remaining entries are zeros. Each row is associated with a comparator which compares the received signal addressed with the position of the 1 with another received signal addressed by the position of the -1. With $\mathbf{B} = \begin{bmatrix} \mathbf{I}_{2N_r}; \mathbf{B}' \end{bmatrix}$, (4) reads as

$$\mathbf{z}_Q = \mathcal{Q}(\mathbf{z}_R) = \mathcal{Q}(\mathbf{B}\mathbf{y}_R). \quad (6)$$

III. CHANNEL ESTIMATION

In this section, we describe pilot-based channel estimation and propose the statistically equivalent linear model for the novel receiver with 1-bit ADCs and the comparator network, which is then utilized for the proposed LRA-MMSE channel estimation. We then characterize the MSE performance associated with the channel estimates.

A. Pilot-Based Channel Estimation and the Proposed Linear Model

A common technique for channel estimation is to let the users transmit orthogonal pilot sequences with length τ and evaluate the effect of the channel on these symbols at the BS. During the training phase, the received signal at the BS can be described by

$$\mathbf{Y}_p = \mathbf{H}\Phi^T + \mathbf{N}_p, \quad (7)$$

where $\mathbf{Y}_p \in \mathbb{C}^{N_r \times \tau}$ is the matrix containing the unquantized received signal, $\Phi \in \mathbb{C}^{\tau \times N_t}$ is the matrix of pilot symbols and $\mathbf{N}_p \in \mathbb{C}^{N_r \times \tau}$ is the noise matrix. Vectorizing the signal in (7) yields

$$\text{vec}(\mathbf{Y}_p) = \mathbf{y}_p = \tilde{\Phi}\mathbf{h} + \mathbf{n}_p, \quad (8)$$

where $\tilde{\Phi} = (\Phi \otimes \mathbf{I}_{N_r}) \in \mathbb{C}^{\tau N_r \times N_r N_t}$, $\mathbf{h} = \text{vec}(\mathbf{H}) \in \mathbb{C}^{N_r N_t \times 1}$ and $\mathbf{n}_p = \text{vec}(\mathbf{N}_p) \in \mathbb{C}^{\tau N_r \times 1}$. A real-valued representation of the system is defined by

$$\mathbf{y}_{R_p} = \begin{bmatrix} \Re\{\tilde{\Phi}\} & -\Im\{\tilde{\Phi}\} \\ \Im\{\tilde{\Phi}\} & \Re\{\tilde{\Phi}\} \end{bmatrix} \begin{bmatrix} \Re\{\mathbf{h}\} \\ \Im\{\mathbf{h}\} \end{bmatrix} + \begin{bmatrix} \Re\{\mathbf{n}_p\} \\ \Im\{\mathbf{n}_p\} \end{bmatrix} = \tilde{\Phi}_R \mathbf{h}_R + \mathbf{n}_{R_p}, \quad (9)$$

where $\mathbf{y}_{R_p} \in \mathbb{R}^{\tau(2N_r) \times 1}$ is the real-valued received signal vector. Then, when we multiply (9) with an effective comparator network matrix $\mathbf{B}_{\text{eff}} \in \mathbb{R}^{\tau(2N_r + \alpha) \times \tau(2N_r)}$, we obtain the vector

$$\mathbf{z}_{R_p} = \mathbf{B}_{\text{eff}}\mathbf{y}_{R_p} = \mathbf{B}_{\text{eff}}\tilde{\Phi}_R \mathbf{h}_R + \mathbf{B}_{\text{eff}}\mathbf{n}_{R_p}, \quad (10)$$

of dimensions $(\tau(2N_r + \alpha) \times 1)$, where \mathbf{B}_{eff} is described by

$$\mathbf{B}_{\text{eff}} = \begin{bmatrix} \mathbf{I}_{\tau(2N_r)} \\ \mathbf{B}'_{\text{eff}} \end{bmatrix} = \begin{bmatrix} \mathbf{I}_{\tau(2N_r)} \\ \begin{bmatrix} \mathbf{B}'_{\text{eff, R}} & \mathbf{B}'_{\text{eff, I}} \end{bmatrix} \end{bmatrix}, \quad (11)$$

with $\mathbf{B}'_{\text{eff}, \text{R}} = (\mathbf{B}'_{\text{R}} \otimes \mathbf{I}_{\tau}) \in \mathbb{R}^{\alpha\tau \times N_r\tau}$ and $\mathbf{B}'_{\text{eff}, \text{I}} = (\mathbf{B}'_{\text{I}} \otimes \mathbf{I}_{\tau}) \in \mathbb{R}^{\alpha\tau \times N_r\tau}$. Moreover, \mathbf{B}'_{R} and \mathbf{B}'_{I} denote the parts of the matrix \mathbf{B}' which are associated to the real and imaginary parts of the received signal, as shown in (5). According to (6), the quantized signal, of dimensions $(\tau(2N_r + \alpha) \times 1)$, is given by

$$\mathbf{z}_{\mathcal{Q}_p} = \mathcal{Q}(\mathbf{z}_{\text{R}_p}) = \hat{\Phi}_{\text{R}} \mathbf{h}_{\text{R}} + \tilde{\mathbf{n}}_{\text{R}_p}, \quad (12)$$

where the right hand side corresponds to a linear model that relies on the Bussgang decomposition approach, and the linear operator is $\hat{\Phi}_{\text{R}} = \mathbf{A}_{\text{R}_p} \mathbf{B}_{\text{eff}} \tilde{\Phi}_{\text{R}} \in \mathbb{R}^{\tau(2N_r + \alpha) \times 2N_r N_t}$. The effective noise vector $\tilde{\mathbf{n}}_{\text{R}_p} = \mathbf{A}_{\text{R}_p} \mathbf{B}_{\text{eff}} \mathbf{n}_{\text{R}_p} + \mathbf{n}_{q,p}$ relies on a well-chosen square matrix $\mathbf{A}_{\text{R}_p} \in \mathbb{R}^{\tau(2N_r + \alpha) \times \tau(2N_r + \alpha)}$ and the quantization noise $\mathbf{n}_{q,p}$. The matrix \mathbf{A}_{R_p} makes the quantization noise uncorrelated with \mathbf{z}_{R_p} [34], and is given by

$$\mathbf{A}_{\text{R}_p} = \mathbf{C}_{\mathbf{z}_{\text{R}_p} \mathbf{z}_{\mathcal{Q}_p}}^H \mathbf{C}_{\mathbf{z}_{\text{R}_p}}^{-1} = \sqrt{\frac{2}{\pi}} \mathbf{K}_{\text{R}_p}, \quad (13)$$

with $\mathbf{K}_{\text{R}_p} = \text{diag}(\mathbf{C}_{\mathbf{z}_{\text{R}_p}})^{-\frac{1}{2}}$. The cross-correlation matrix between the received signal \mathbf{z}_{R_p} and its quantized signal $\mathbf{z}_{\mathcal{Q}_p}$, of dimensions $(\tau(2N_r + \alpha) \times (\tau(2N_r + \alpha)))$, reads as

$$\mathbf{C}_{\mathbf{z}_{\text{R}_p} \mathbf{z}_{\mathcal{Q}_p}} = \sqrt{\frac{2}{\pi}} \mathbf{K}_{\text{R}_p} \mathbf{C}_{\mathbf{z}_{\text{R}_p}}. \quad (14)$$

The matrix $\mathbf{C}_{\mathbf{z}_{\text{R}_p}}$, of dimensions $(\tau(2N_r + \alpha) \times (\tau(2N_r + \alpha)))$, denotes the auto-correlation matrix of \mathbf{z}_{R_p}

$$\mathbf{C}_{\mathbf{z}_{\text{R}_p}} = \mathbf{B}_{\text{eff}} (\tilde{\Phi}_{\text{R}} \mathbf{R}_{\text{h}_R} \tilde{\Phi}_{\text{R}}^T + \frac{1}{2} \sigma_n^2 \mathbf{I}_{\tau(2N_r)}) \mathbf{B}_{\text{eff}}^T, \quad (15)$$

where $\mathbf{R}_{\text{h}_R} = E[\mathbf{h}_{\text{R}} \mathbf{h}_{\text{R}}^T]$. In (15) it is considered $E[\mathbf{n}_{\text{R}_p} \mathbf{n}_{\text{R}_p}^T] = \frac{1}{2} \sigma_n^2 \mathbf{I}_{\tau(2N_r)}$, due to noise samples in real-valued notation with variance $\frac{1}{2} \sigma_n^2$. Note that knowledge about \mathbf{R}_{h_R} might not be available at the receiver. For this case, a sample channel correlation matrix can be estimated based on 1-bit measurements using the method devised in [23]. Assuming that the channel is a Rayleigh fading channel without spatial correlation implies $\mathbf{R}_{\text{h}_R} = \frac{1}{2} \mathbf{I}$. For this case (15) simplifies to

$$\mathbf{C}_{\mathbf{z}_{\text{R}_p}} = \mathbf{B}_{\text{eff}} \left(\frac{1}{2} \tilde{\Phi}_{\text{R}} \tilde{\Phi}_{\text{R}}^T + \frac{1}{2} \sigma_n^2 \mathbf{I}_{2\tau N_r} \right) \mathbf{B}_{\text{eff}}^T. \quad (16)$$

Considering that $\tau = N_t$ we have $\tilde{\Phi}_{\text{R}} \tilde{\Phi}_{\text{R}}^T = N_t \sigma_x^2 \mathbf{I}_{2\tau N_r}$ which yields

$$\mathbf{C}_{\mathbf{z}_{\text{R}_p}} = \mathbf{B}_{\text{eff}} \left(\frac{1}{2} N_t \sigma_x^2 \mathbf{I}_{2\tau N_r} + \frac{1}{2} \sigma_n^2 \mathbf{I}_{2\tau N_r} \right) \mathbf{B}_{\text{eff}}^T. \quad (17)$$

This can be written more compactly as

$$\mathbf{C}_{\mathbf{z}_{\text{R}_p}} = \frac{1}{2} (N_t \sigma_x^2 + \sigma_n^2) \mathbf{B}_{\text{eff}} \mathbf{B}_{\text{eff}}^T. \quad (18)$$

The matrix $\mathbf{B}_{\text{eff}}\mathbf{B}_{\text{eff}}^T$ has only ones on its diagonal. With this, one can conclude that

$$\mathbf{A}_{\mathbf{R}_p} = \sqrt{\frac{2}{\pi} \frac{2}{N_t \sigma_x^2 + \sigma_n^2}} \mathbf{I}_{\tau(2N_r + \alpha)}. \quad (19)$$

B. Proposed LRA-LMMSE Channel Estimator

Employing the proposed statistically equivalent linear model in (12) allows the adoption of the established technique for linear channel estimation with quantization error [19], [20], [23]. Based on (12) the LRA-LMMSE estimator can be obtained through the optimization problem formulated as

$$\mathbf{W}_{\mathbf{R}, \text{LRA-LMMSE}} = \arg \min_{\mathbf{W}} E \left[\|\mathbf{h}_{\mathbf{R}} - \mathbf{W}\mathbf{z}_{\mathcal{Q}_p}\|_2^2 \right] = \mathbf{R}_{\mathbf{h}_{\mathbf{R}}} \hat{\Phi}_{\mathbf{R}}^T \mathbf{C}_{\mathbf{z}_{\mathcal{Q}_p}}^{-1}, \quad (20)$$

where the auto-correlation of the quantized signal is calculated as [35]

$$\mathbf{C}_{\mathbf{z}_{\mathcal{Q}_p}} = \frac{2}{\pi} \sin^{-1} \left(\mathbf{K}_{\mathbf{R}_p} \mathbf{C}_{\mathbf{z}_{\mathbf{R}_p}} \mathbf{K}_{\mathbf{R}_p} \right). \quad (21)$$

For the Rayleigh fading channel with $\mathbf{R}_{\mathbf{h}_{\mathbf{R}}} = \frac{1}{2} \mathbf{I}_{2N_t N_r}$ and $\tau = N_t$ we have

$$\mathbf{C}_{\mathbf{z}_{\mathcal{Q}_p}} = \frac{2}{\pi} \sin^{-1} \left(\mathbf{B}_{\text{eff}} \mathbf{B}_{\text{eff}}^T \right) \approx \frac{2}{\pi} \left(\mathbf{B}_{\text{eff}} \mathbf{B}_{\text{eff}}^T + \left(\frac{\pi}{2} - 1 \right) \mathbf{I}_{2\tau N_r} \right) = \frac{\pi - 2}{\pi} \left(\frac{2}{(\pi - 2)} \mathbf{B}_{\text{eff}} \mathbf{B}_{\text{eff}}^T + \mathbf{I}_{2\tau N_r} \right). \quad (22)$$

The resulting LRA-LMMSE channel estimator is given by

$$\hat{\mathbf{h}}_{\mathbf{R}, \text{LRA-LMMSE}} = \begin{bmatrix} \hat{\mathbf{h}}_{\mathbf{R}, \text{LRA-LMMSE}, a} \\ \hat{\mathbf{h}}_{\mathbf{R}, \text{LRA-LMMSE}, b} \end{bmatrix} = \mathbf{W}_{\mathbf{R}, \text{LRA-LMMSE}} \mathbf{z}_{\mathcal{Q}_p}, \quad (23)$$

where $\hat{\mathbf{h}}_{\mathbf{R}, \text{LRA-LMMSE}, a} \in \mathbb{R}^{N_r N_t \times 1}$ is the first half of the channel estimate which corresponds to the real part and $\hat{\mathbf{h}}_{\mathbf{R}, \text{LRA-LMMSE}, b} \in \mathbb{R}^{N_r N_t \times 1}$ is the second half which corresponds to the imaginary part. A detailed derivation is shown in Appendix A.

C. Error Correlation Matrix and MSE of the Channel Estimate

Inserting the estimated channel vector in the cost function of the MSE problem (20) yields

$$\mathcal{M}_{\mathbf{R}, \text{LRA-MMSE}} = E \left[\left\| \mathbf{h}_{\mathbf{R}} - \hat{\mathbf{h}}_{\mathbf{R}, \text{LRA-MMSE}} \right\|_2^2 \right] \quad (24)$$

$$= \text{tr} \left(E \left[\epsilon_{\mathbf{R}} \epsilon_{\mathbf{R}}^T \right] \right), \quad (25)$$

with $\epsilon_{\mathbf{R}} = \mathbf{h}_{\mathbf{R}} - \hat{\mathbf{h}}_{\mathbf{R}, \text{LRA-MMSE}}$. The channel estimation error correlation matrix is then given by

$$E \left[\epsilon_{\mathbf{R}} \epsilon_{\mathbf{R}}^T \right] = E \left[\hat{\mathbf{h}}_{\mathbf{R}, \text{LRA-MMSE}} \hat{\mathbf{h}}_{\mathbf{R}, \text{LRA-MMSE}}^T - 2\hat{\mathbf{h}}_{\mathbf{R}, \text{LRA-MMSE}} \mathbf{h}_{\mathbf{R}}^T + \mathbf{h}_{\mathbf{R}} \mathbf{h}_{\mathbf{R}}^T \right]. \quad (26)$$

By inserting (23) and (12) into (26), and considering that \mathbf{h}_R is uncorrelated with $\tilde{\mathbf{n}}_{R,p}$, the error correlation matrix can be expressed as

$$E [\epsilon_R \epsilon_R^T] = \mathbf{R}_{h_R} - \mathbf{R}_{h_R} \hat{\Phi}_R^T \mathbf{C}_{z_{Q,p}}^{-1} \hat{\Phi}_R \mathbf{R}_{h_R}. \quad (27)$$

Note that the channel estimation correlation matrix can be taken into account for robust detection as presented in Section IV-C. The corresponding expression for the MSE is given by

$$\mathcal{M}_{R, \text{LRA-MMSE}} = \text{tr} \left(\mathbf{R}_{h_R} - \mathbf{R}_{h_R} \hat{\Phi}_R^T \mathbf{C}_{z_{Q,p}}^{-1} \hat{\Phi}_R \mathbf{R}_{h_R} \right). \quad (28)$$

The correlation matrix of the channel estimate is given by

$$E \left[\hat{\mathbf{h}}_{R, \text{LRA-MMSE}} \hat{\mathbf{h}}_{R, \text{LRA-MMSE}}^T \right] = \mathbf{R}_{h_R} \hat{\Phi}_R^T \mathbf{C}_{z_{Q,p}}^{-1} \hat{\Phi}_R \mathbf{R}_{h_R}. \quad (29)$$

By using the approximation in (22) for $\mathbf{C}_{z_{Q,p}}^{-1}$ the correlation matrix can be expressed as

$$E \left[\hat{\mathbf{h}}_{R, \text{LRA-MMSE}} \hat{\mathbf{h}}_{R, \text{LRA-MMSE}}^T \right] = \frac{\pi}{\pi - 2} \mathbf{R}_{h_R} \hat{\Phi}_R^T \left(\frac{2}{\pi - 2} \mathbf{B}_{\text{eff}} \mathbf{B}_{\text{eff}}^T + \mathbf{I} \right)^{-1} \hat{\Phi}_R \mathbf{R}_{h_R}. \quad (30)$$

By considering $\mathbf{R}_{h_R} = \frac{1}{2} \mathbf{I}$ and $\tau = N_t$, (19) can be applied and the correlation matrix of the channel estimate reads as

$$E \left[\hat{\mathbf{h}}_{R, \text{LRA-MMSE}} \hat{\mathbf{h}}_{R, \text{LRA-MMSE}}^T \right] = \frac{1}{4} \frac{2}{\pi} \frac{2}{N_t \sigma_x^2 + \sigma_n^2} \frac{\pi}{\pi - 2} \tilde{\Phi}_R^T \mathbf{B}_{\text{eff}}^T \left(\frac{2}{\pi - 2} \mathbf{B}_{\text{eff}} \mathbf{B}_{\text{eff}}^T + \mathbf{I} \right)^{-1} \mathbf{B}_{\text{eff}} \tilde{\Phi}_R. \quad (31)$$

Using the push-through identity one can write

$$E \left[\hat{\mathbf{h}}_{R, \text{LRA-MMSE}} \hat{\mathbf{h}}_{R, \text{LRA-MMSE}}^T \right] = \frac{1}{N_t \sigma_x^2 + \sigma_n^2} \frac{1}{\pi - 2} \tilde{\Phi}_R^T \mathbf{B}_{\text{eff}}^T \mathbf{B}_{\text{eff}} \left(\frac{2}{\pi - 2} \mathbf{B}_{\text{eff}} \mathbf{B}_{\text{eff}}^T + \mathbf{I} \right)^{-1} \tilde{\Phi}_R. \quad (32)$$

In the following it is considered that the diagonal elements in the matrix $\mathbf{B}_{\text{eff}}^T \mathbf{B}_{\text{eff}}$ are much larger than the off diagonal elements. Considering $\mathbf{B}_{\text{eff}}^T \mathbf{B}_{\text{eff}} \approx \text{diag} [b_1, b_2 \dots b_{\tau 2N_r}]$ yields

$$E \left[\hat{\mathbf{h}}_{R, \text{LRA-MMSE}} \hat{\mathbf{h}}_{R, \text{LRA-MMSE}}^T \right] = \frac{1}{N_t \sigma_x^2 + \sigma_n^2} \frac{1}{2} \tilde{\Phi}_R^T \left(\mathbf{I}_{\tau 2N_r} - (\pi - 2) \text{diag} \left[\frac{1}{2b_1 + \pi - 2}, \frac{1}{2b_2 + \pi - 2} \dots \frac{1}{2b_{\tau 2N_r} + \pi - 2} \right] \right) \tilde{\Phi}_R. \quad (33)$$

For a comparator network matrix with uniformly distributed non-zero entries, the probability of a non-zero at any position in matrix B'_{eff} is equal to $\frac{1}{N_r \tau}$. Accordingly it holds $E [|B'_{\text{eff},i,j}|^2] = \frac{1}{N_r \tau} \frac{1}{2}$, which implies $E [\mathbf{B}_{\text{eff}}^T \mathbf{B}_{\text{eff}}] = (1 + \frac{\alpha}{2N_r}) \mathbf{I}$ and $E [b_i] = 1 + \frac{\alpha}{2N_r}$. By replacing b_i by its expected value, (33) is approximated by

$$E \left[\hat{\mathbf{h}}_{R, \text{LRA-MMSE}} \hat{\mathbf{h}}_{R, \text{LRA-MMSE}}^T \right] = \frac{1}{N_t \sigma_x^2 + \sigma_n^2} \frac{1}{2} \left(1 - \frac{\pi - 2}{2(1 + \frac{\alpha}{2N_r}) + \pi - 2} \right) \tilde{\Phi}_R^T \tilde{\Phi}_R. \quad (34)$$

Finally, with $\tilde{\Phi}_R^T \tilde{\Phi}_R = N_t \sigma_x^2 \mathbf{I}$, it holds

$$E \left[\hat{\mathbf{h}}_{R, \text{LRA-MMSE}} \hat{\mathbf{h}}_{R, \text{LRA-MMSE}}^T \right] = \frac{1}{2} \frac{N_t \sigma_x^2}{N_t \sigma_x^2 + \sigma_n^2} \left(1 - \frac{\pi - 2}{2(1 + \frac{\alpha}{2N_r}) + \pi - 2} \right) \mathbf{I}_{2N_r N_t}. \quad (35)$$

In the following a short hand notation for the prefactor in (35) will be used in terms of κ . With this, the sum MSE can be approximated as $\mathcal{M}_{R, \text{LRA-MMSE}} = N_r N_t (1 - 2\kappa)$.

IV. LINEAR DETECTION

In this section, we present linear detection techniques based on comparator networks. In particular, we describe the proposed LRA-LMMSE detector for perfect (or near perfect) CSI scenarios and the proposed robust LRA-LMMSE detector for scenarios with imperfect CSI. To the best of the authors knowledge, the proposed study is the first to deal with a robust approach for 1-bit MIMO receivers.

A. Proposed LRA-LMMSE Detector for Perfect CSI

Based on the proposed system model in (6), the corresponding linear receiver to estimate the transmitted symbols is derived as follows. The optimization problem that yields the linear optimal receiver reads as

$$\mathbf{G}_{R, \text{LRA-MMSE}} = \arg \min_{\mathbf{G}_R} E \left[\|\mathbf{x}_R - \mathbf{G}_R^T \mathbf{z}_Q\|_2^2 \right], \quad (36)$$

where $\mathbf{G}_R \in \mathbb{R}^{(2N_r + \alpha) \times 2N_t}$. The solution for (36) is given by

$$\mathbf{G}_{R, \text{LRA-MMSE}} = \mathbf{C}_{\mathbf{z}_Q}^{-1} \mathbf{C}_{\mathbf{z}_Q \mathbf{x}_R}, \quad (37)$$

where the involved covariance matrix $\mathbf{C}_{\mathbf{z}_Q}$ is calculated as [35]

$$\mathbf{C}_{\mathbf{z}_Q} = \frac{2}{\pi} \sin^{-1} (\mathbf{K}_R \mathbf{C}_{\mathbf{z}_R} \mathbf{K}_R), \quad (38)$$

and the cross-correlation matrix $\mathbf{C}_{\mathbf{z}_Q \mathbf{x}_R}$ is based on the Bussgang theorem [36]

$$\mathbf{C}_{\mathbf{z}_Q \mathbf{x}_R} = \sqrt{\frac{2}{\pi}} \frac{\sigma_x^2}{2} \mathbf{K}_R \mathbf{B} \mathbf{H}_R, \quad (39)$$

with $\mathbf{K}_R = \text{diag}(\mathbf{C}_{\mathbf{z}_R})^{-\frac{1}{2}} \in \mathbb{R}^{(2N_r + \alpha) \times (2N_r + \alpha)}$. The cross-correlation matrix between \mathbf{z}_R and \mathbf{x}_R is given by

$$\mathbf{C}_{\mathbf{z}_R \mathbf{x}_R} = \frac{1}{2} \sigma_x^2 \mathbf{B} \mathbf{H}_R, \quad (40)$$

where due to the real-valued notation of the system the input correlation matrix is given by $\mathbf{C}_{\mathbf{x}_R} = E[\mathbf{x}_R \mathbf{x}_R^T] = \frac{1}{2} \sigma_x^2 \mathbf{I}_{2N_t}$. Besides, the correlation matrix of \mathbf{z}_R is given by

$$\mathbf{C}_{\mathbf{z}_R} = \frac{1}{2} \sigma_x^2 \mathbf{B} \mathbf{H}_R \mathbf{H}_R^T \mathbf{B}^T + \frac{1}{2} \sigma_n^2 \mathbf{B} \mathbf{B}^T, \quad (41)$$

where the noise correlation matrix is given by $\mathbf{C}_{\mathbf{n}_R} = E[\mathbf{n}_R \mathbf{n}_R^T] = \frac{1}{2} \sigma_n^2 \mathbf{I}_{2N_r}$, which is due to the real-valued notation of the system.

B. Robust LRA-LMMSE Detector for Imperfect CSI

In this subsection, a robust LRA-MMSE detector is proposed, which takes into account statistics of CSI imperfections. In this context, it is considered that the channel can be described by two uncorrelated terms as $\mathbf{h}_R = \sqrt{\lambda} \mathbf{h}_{R,1} + \sqrt{1-\lambda} \mathbf{h}_{R,2}$, where $\mathbf{h}_{R,1}$, λ and the correlation matrix $\mathbf{R}_{\mathbf{h}_{R,2}} = E[\mathbf{h}_{R,2} \mathbf{h}_{R,2}^T]$ are considered to be known at the receiver. The quality of the CSI is determined by parameter $0 < \lambda < 1$.

As an example, this model could represent a time-varying channel with wide-sense stationarity and known temporal autocorrelation function, similar to the assumptions used in [23]. In this case, $\mathbf{h}_{R,1}$ is an outdated channel vector and $\sqrt{\lambda}$ represents the value of the temporal channel autocorrelation function, where we assume the same properties for all users.

Based on this model, we redefine the received signal as

$$\begin{aligned} \mathbf{y}_R &= \begin{bmatrix} \Re\{\tilde{\mathbf{X}}\} & -\Im\{\tilde{\mathbf{X}}\} \\ \Im\{\tilde{\mathbf{X}}\} & \Re\{\tilde{\mathbf{X}}\} \end{bmatrix} \begin{bmatrix} \Re\{\mathbf{h}\} \\ \Im\{\mathbf{h}\} \end{bmatrix} + \begin{bmatrix} \Re\{\mathbf{n}_d\} \\ \Im\{\mathbf{n}_d\} \end{bmatrix} \\ &= \sqrt{\lambda} \mathbf{H}_{R,1} \mathbf{x}_R + \sqrt{1-\lambda} \tilde{\mathbf{X}}_R \mathbf{h}_{R,2} + \mathbf{n}_{R,d}, \end{aligned} \quad (42)$$

where $\mathbf{y}_R \in \mathbb{R}^{2N_r \times 1}$ and $\tilde{\mathbf{X}} = (\mathbf{x}^T \otimes \mathbf{I}_{N_r}) \in \mathbb{C}^{N_r \times N_t N_r}$. The subscript d refers to data. Moreover, $\mathbf{H}_{R,1} \in \mathbb{R}^{2N_r \times 2N_t}$ is the known part of the channel matrix, described by

$$\begin{aligned} \mathbf{H}_{R,1} &= \begin{bmatrix} \Re\{\mathbf{H}_1\} & -\Im\{\mathbf{H}_1\} \\ \Im\{\mathbf{H}_1\} & \Re\{\mathbf{H}_1\} \end{bmatrix} \text{ with } \mathbf{H}_1 = \text{unvec}(\mathbf{h}_1) \\ \text{and } \mathbf{h}_1 &= [\mathbf{h}_{R,1,a} + j\mathbf{h}_{R,1,b}], \end{aligned} \quad (43)$$

where $\mathbf{h}_{R,1,a}$ corresponds to the first half of the known part $\mathbf{h}_{R,1}$ and $\mathbf{h}_{R,1,b}$ to the second half. With this, the quantized signal of the comparator aided MIMO receiver can be expressed as

$$\mathbf{z}_{Q_r} = \mathcal{Q}(\mathbf{z}_{R_r}) = \sqrt{\lambda} \mathbf{A}_{R_r} \mathbf{B} \mathbf{H}_{R,1} \mathbf{x}_R + \sqrt{1-\lambda} \mathbf{A}_{R_r} \mathbf{B} \tilde{\mathbf{X}}_R \mathbf{h}_{R,2} + \mathbf{A}_{R_r} \mathbf{B} \mathbf{n}_{R,d} + \mathbf{n}_{R_q,d}, \quad (44)$$

of dimensions $(2N_r + \alpha) \times 1$, where \mathbf{A}_{R_r} is the Bussgang-based linear operator for the transmit data, similarly as calculated in (13). Then, the LRA-LMMSE filter is applied to \mathbf{z}_{Q_r} , to obtain

$$\hat{\mathbf{x}}_R = \mathbf{G}_R^T \mathbf{z}_{Q_r}, \quad (45)$$

where the matrix $\mathbf{G}_R \in \mathbb{R}^{(2N_r + \alpha) \times 2N_t}$ is chosen to minimize the MSE between the transmitted symbol \mathbf{x}_R and the filter output, i.e.,

$$\begin{aligned} \tilde{\mathbf{G}}_{R, \text{LRA-MMSE}} &= \arg \min_{\mathbf{G}_R} E \left[\left\| \mathbf{x}_R - \mathbf{G}_R^T \mathbf{z}_{Q_r} \right\|_2^2 \right] \\ &= \arg \min_{\mathbf{G}_R} -2\text{tr} \left(\mathbf{G}_R^T \mathbf{C}_{\mathbf{z}_{Q_r}, \mathbf{x}_R} \right) + \text{tr} \left(\mathbf{G}_R^T \mathbf{C}_{\mathbf{z}_{Q_r}} \mathbf{G}_R \right), \end{aligned} \quad (46)$$

where the latter describes an equivalent problem. By differentiating (46) with respect to \mathbf{G}_R^T and equating it to zero, the solution of the LRA-LMMSE receive filter is given by

$$\tilde{\mathbf{G}}_{R, \text{LRA-MMSE}} = \mathbf{C}_{\mathbf{z}_{Q_r}}^{-1} \mathbf{C}_{\mathbf{z}_{Q_r}, \mathbf{x}_R}. \quad (47)$$

As in the previous cases, the covariance matrix, of dimensions $(2N_r + \alpha) \times (2N_r + \alpha)$, is calculated as [35]

$$\mathbf{C}_{\mathbf{z}_{Q_r}} = \frac{2}{\pi} \sin^{-1} \left(\mathbf{K}_{R_r} \mathbf{C}_{\mathbf{z}_{R_r}} \mathbf{K}_{R_r} \right), \quad (48)$$

and the cross-correlation matrix, of dimensions $(2N_r + \alpha) \times 2N_t$, is based on the Bussgang theorem [36]

$$\mathbf{C}_{\mathbf{z}_{Q_r}, \mathbf{x}_R} = \sqrt{\frac{2}{\pi}} \frac{\sigma_x^2}{2} \mathbf{K}_{R_r} \mathbf{B} \mathbf{H}_{R,1}, \quad (49)$$

with $\mathbf{K}_{R_r} = \text{diag}(\mathbf{C}_{\mathbf{z}_{R_r}})^{-\frac{1}{2}}$ and the cross-correlation matrix between \mathbf{z}_{R_r} and \mathbf{x}_R , of dimensions $(2N_r + \alpha) \times 2N_t$, is given by $\mathbf{C}_{\mathbf{z}_{R_r}, \mathbf{x}_R} = \frac{1}{2} \sigma_x^2 \mathbf{B} \mathbf{H}_{R,1}$, where due to the real-valued notation of the system the input correlation matrix $\mathbf{C}_{\mathbf{x}_R} = E[\mathbf{x}_R \mathbf{x}_R^T] = \frac{1}{2} \sigma_x^2 \mathbf{I}_{2N_t}$ is considered. Moreover, the correlation matrix of the unquantized output signal \mathbf{z}_{R_r} is given by

$$\mathbf{C}_{\mathbf{z}_{R_r}} = \lambda \frac{1}{2} \sigma_x^2 \mathbf{B} \mathbf{H}_{R,1} \mathbf{H}_{R,1}^T \mathbf{B}^T + (1 - \lambda) \mathbf{B} \mathbf{\Gamma}_R \mathbf{B}^T + \frac{1}{2} \sigma_n^2 \mathbf{B} \mathbf{B}^T. \quad (50)$$

The matrix $\mathbf{\Gamma}_R \in \mathbb{R}^{N_r N_t \times N_r N_t}$ in (50) is calculated as follows:

$$\mathbf{\Gamma}_R = E \left[\tilde{\mathbf{X}}_R \mathbf{R}_{\mathbf{h}_{R,2}} \tilde{\mathbf{X}}_R^T \right]. \quad (51)$$

In the following it is considered that the transmit symbols are taken from an M_x -ary symbol alphabet and that the prior probabilities are known at the receiver. With this, the expected value in (51) can be calculated as

$$\mathbf{\Gamma}_R = \sum_{i=1}^{M_x^{N_t}} P \left(\tilde{\mathbf{X}}_{R,i} \right) \left(\tilde{\mathbf{X}}_{R,i} \mathbf{R}_{\mathbf{h}_{R,2}} \tilde{\mathbf{X}}_{R,i}^T \right), \quad (52)$$

where $P \left(\tilde{\mathbf{X}}_{R,i} \right) = \frac{1}{4^{N_t}}$ in case of uniformly distributed QPSK transmit symbols.

C. Robust LRA-LMMSE Detector for Imperfect CSI Caused by Channel Estimation

The robust detector described in the previous section can be applied to the case of imperfect channel estimation caused by channel estimation. In this case, we substitute the channel description from the previous section in terms of $\sqrt{\lambda}\mathbf{h}_{R,1} = \hat{\mathbf{h}}_R$ and $\sqrt{1-\lambda}\mathbf{h}_{R,2} = \boldsymbol{\varepsilon}_R$. With this, the cross-correlation matrix, of dimensions $(2N_r + \alpha) \times 2N_t$, is given by [36]

$$\mathbf{C}_{\mathbf{z}_{Q_r}, \mathbf{x}_R} = \sqrt{\frac{2}{\pi}} \frac{\sigma_x^2}{2} \mathbf{K}_{R_r} \mathbf{B} \hat{\mathbf{H}}_R, \quad (53)$$

with $\mathbf{K}_{R_r} = \text{diag}(\mathbf{C}_{\mathbf{z}_{R_r}})^{-\frac{1}{2}}$. The cross-correlation matrix between \mathbf{z}_{R_r} and \mathbf{x}_R reads as $\mathbf{C}_{\mathbf{z}_{R_r}, \mathbf{x}_R} = \frac{1}{2} \sigma_x^2 \mathbf{B} \hat{\mathbf{H}}_R$. Moreover, the correlation matrix of the unquantized output signal \mathbf{z}_{R_r} is given by

$$\mathbf{C}_{\mathbf{z}_{R_r}} = \frac{1}{2} \sigma_x^2 \mathbf{B} \hat{\mathbf{H}}_R \hat{\mathbf{H}}_R^T \mathbf{B}^T + \mathbf{B} \boldsymbol{\Gamma}_R \mathbf{B}^T + \frac{1}{2} \sigma_n^2 \mathbf{B} \mathbf{B}^T. \quad (54)$$

The matrix $\boldsymbol{\Gamma}_R$ in (54) is calculated as follows

$$\boldsymbol{\Gamma}_R = E \left[\tilde{\mathbf{X}}_R E \left[\boldsymbol{\varepsilon}_R \boldsymbol{\varepsilon}_R^T \right] \tilde{\mathbf{X}}_R^T \right] = E \left[\tilde{\mathbf{X}}_R \mathbf{R}_{\text{hr}} \tilde{\mathbf{X}}_R^T - \tilde{\mathbf{X}}_R \mathbf{R}_{\text{hr}} \hat{\boldsymbol{\Phi}}_R^T \mathbf{C}_{\mathbf{z}_{Q_p}}^{-1} \hat{\boldsymbol{\Phi}}_R \mathbf{R}_{\text{hr}} \tilde{\mathbf{X}}_R^T \right], \quad (55)$$

where the matrix $E \left[\boldsymbol{\varepsilon}_R \boldsymbol{\varepsilon}_R^T \right]$ depends on the considered channel estimation method. For the proposed channel estimation in the section III the matrix is given by $E \left[\boldsymbol{\varepsilon}_R \boldsymbol{\varepsilon}_R^T \right] = \mathbf{R}_{\text{hr}} - \mathbf{R}_{\text{hr}} \hat{\boldsymbol{\Phi}}_R^T \mathbf{C}_{\mathbf{z}_{Q_p}}^{-1} \hat{\boldsymbol{\Phi}}_R \mathbf{R}_{\text{hr}}$, which is related to previously calculated MSE expression (28).

V. DESIGN OF THE COMPARATOR NETWORK

The matrix design of the comparator network in (5) is detailed in this section. Two types of networks are considered, namely, fully and partially connected networks.

A. Fully Connected Network

In this network, every two of the received signals are compared, which means that the number of comparators is $\alpha_f = \binom{2N_r}{2} = N_r(2N_r - 1)$. For instance, if we consider a system with $N_r = 2$ receive antennas, $\alpha_f = \binom{4}{2} = 6$ comparators are needed in this network. Then, the corresponding matrix \mathbf{B}' is described by

$$\mathbf{B}'_{\alpha_f} = \frac{1}{\sqrt{2}} \begin{bmatrix} 1 & -1 & 0 & 0 \\ 1 & 0 & -1 & 0 \\ 1 & 0 & 0 & -1 \\ 0 & 1 & -1 & 0 \\ 0 & 1 & 0 & -1 \\ 0 & 0 & 1 & -1 \end{bmatrix}. \quad (56)$$

The main drawback of the fully connected network is the massive use of the comparators, where the number of comparators α_f is approximately proportional to the square of the number of receive antennas N_r . Therefore, in large-scale multiuser MIMO systems a much larger number of comparators will be required, which might be unrealistic.

B. Partially Connected Network

In order to increase the usage efficiency of the comparators, the partially connected network is proposed, where the number of utilized comparators α_p is only a small fraction of the number of comparators in the fully connected network. For the same scenario described in the previous subsection, one possibility for the corresponding matrix \mathbf{B}'_{α_p} can be described by

$$\mathbf{B}'_{\alpha_p} = \frac{1}{\sqrt{2}} \begin{bmatrix} 1 & -1 & 0 & 0 \\ 1 & 0 & -1 & 0 \\ 1 & 0 & 0 & -1 \\ 0 & 1 & -1 & 0 \end{bmatrix}. \quad (57)$$

Different types of network design are considered, namely random, greedy search based and sequentially SINR search based. The random comparator network design randomly selects α_p out of α_f comparator input combinations. The design of the partially connected comparator network in general is a combinatorial problem. For a comparator network consisting of α_p comparators $\binom{N_r(2N_r-1)}{\alpha_p}$ different configurations exist. Two sophisticated search based comparator network designs are developed in the following subsections.

Algorithm 1 MMSE based Greedy Search

- 1: Find the fully connected network \mathbf{B}' in (56) and get the number of rows, defined by α_f
 - 2: Extract the first α_p rows of \mathbf{B}' , defined by \mathbf{B}'_{α_p}
 - 3: Constitute \mathbf{B} in (6) and calculate \mathbf{G}_R in (37)
 - 4: Compute the MSE with $E[\|\mathbf{x}_R - \mathbf{G}_R \mathbf{z}_Q\|_2^2]$, defined by l_{\min}
 - 5: **for** $i = 1 : \alpha_p$ **do**
 - 6: Take the i th row of \mathbf{B}'_{α_p} and freeze the other $\alpha_p - 1$ rows
 - 7: **for** $j = 1 : \alpha_f$ **do**
 - 8: **if** the j th row of \mathbf{B}' is already in \mathbf{B}'_{α_p} **then**
 - 9: $j = j + 1$
 - 10: **else**
 - 11: Replace the i th row of \mathbf{B}'_{α_p} with the j th row of \mathbf{B}'
 - 12: Constitute \mathbf{B} and calculate \mathbf{G}_R
 - 13: Compute the MSE value, defined by l
 - 14: **if** $l < l_{\min}$ **then**
 - 15: $l_{\min} = l$
 - 16: Update \mathbf{B}'_{α_p}
 - 17: **end if**
 - 18: **end if**
 - 19: **end for**
 - 20: **end for**
-

C. Greedy Search Algorithm

The proposed Greedy Search algorithm implies that in each iteration, the comparator input combination with the highest MSE reduction is selected. In a nutshell, the proposed algorithm searches for each individual comparator sequentially over all possible combinations for the minimum MSE input combination. In this process, the comparators sequentially change their inputs according to the MSE criterion. The detailed process is summarized in Algorithm 1.

D. Sequential SINR based Search

The SINR before the quantization operation for the output signal of comparator l with respect to the k th real-valued channel input is described by

$$\text{SINR}_{l,k} = \frac{\frac{1}{2}\sigma_x^2 |[\mathbf{B}'\mathbf{H}_R]_{l,k}|^2}{\frac{1}{2}\sigma_x^2 \sum_{j=1, j \neq k}^{2N_t} |[\mathbf{B}'\mathbf{H}_R]_{l,j}|^2 + \sigma_n^2}. \quad (58)$$

Moreover, the MSE of the k th real valued signal stream after filtering with \mathbf{G}_R reads as

$$\text{MSE}_k = [\mathbf{G}_R^T \mathbf{C}_{\mathbf{z}_Q} \mathbf{G}_R - 2\mathbf{G}_R^T \mathbf{C}_{\mathbf{z}_Q \mathbf{x}_R} + \mathbf{C}_{\mathbf{x}_R}]_{k,k}. \quad (59)$$

The proposed sequential SINR search based comparator network with α_p comparators is sequentially constructed in α_p steps. Implicitly, the objective of the sequential construction is the minimization of the maximum MSE associated with the $2N_t$ signal streams. In each of the α_p steps the algorithm computes the MSE values for each real-valued signal stream based on the current state of the comparator network in combination with an appropriate receive filter. Based on these MSE values, the weakest signal stream is identified where the corresponding index is denoted as k_{max} . Subsequently, the SINR values of all possible comparator output signals with respect to the signal stream k_{max} are considered, namely $\text{SINR}_{k_{max},l}$ for $l \in \mathcal{L}$, where \mathcal{L} denotes the set of comparators, that are not included in the sequentially constructed comparator network. The index associated with the maximum SINR is denoted as $l_{max} = \text{argmax}_{l \in \mathcal{L}} \text{SINR}_{k_{max},l}$. Then the comparator network is extended by the comparator combination with index l_{max} which corresponds to the highest SINR value for the weakest stream k_{max} in terms of MSE. The detailed process for the construction of a network with α comparators is summarized in Algorithm 2.

Algorithm 2 Sequential SINR based Search

- 1: Define the matrix \mathbf{B}' (56) for the fully connected network and compute the number of rows α_f
 - 2: Define the set $\mathcal{L} = \{1, \dots, \alpha_f\}$
 - 3: Compute $\text{SINR}_{l,k}$ for all k and l according to (58).
 - 4: For initialization consider the system without the comparator network with $\mathbf{B} = \mathbf{I}_{2N_r}$.
 - 5: **for** $i = 1 : \alpha_p$ **do**
 - 6: Compute \mathbf{G}_R in (37) due to \mathbf{B}
 - 7: Compute MSE_k for the $2K$ signal streams with (59)
 - 8: Find the index of the weakest signal $k_{\max} = \text{argmax}_k \text{MSE}_k$
 - 9: Find the index of the unused comparator in \mathbf{B}' with the maximum SINR w.r.t. k_{\max}
 - 10: $l_{\max} = \text{argmax}_{l \in \mathcal{L}} \text{SINR}_{k_{\max}, l}$
 - 11: Extend the comparator network matrix with the l_{\max} th row of \mathbf{B}'
 - 12: $\mathbf{B} = \begin{bmatrix} \mathbf{B} \\ \mathbf{B}'_{l_{\max}} \end{bmatrix}$
 - 13: Update the set of unused comparators $\mathcal{L} = \{1, \dots, l_{\max} - 1, l_{\max} + 1, \dots, \alpha_f\}$
 - 14: **end for**
-

VI. COST ANALYSIS AND POWER CONSUMPTION

In this section, we carry out an analysis of the cost and the power consumption of the proposed comparator network aided receivers.

A. Cost Analysis

The corresponding complexity orders are summarized in Table I, where $\mathcal{O}(\cdot)$ is the big O notation. Note that the complexity order can be calculated as functions of the numbers of receive and transmit antennas N_r and N_t and additional comparators α_f or α_p . The required computational

TABLE I: Computational Complexity

Approach	Network Design	LRA-MMSE Detection
No Network	-	$\mathcal{O}((2N_r)^3 + 2N_t(2N_r)^2 + 4N_r N_t)$
Full Connection	-	$\mathcal{O}((2N_r + \alpha_f)^3 + 2N_t(2N_r + \alpha_f)^2 + 2N_t(2N_r + \alpha_f))$
MMSE based Greedy Search	$\mathcal{O}(\alpha_p(\alpha_f - \alpha_p)(2N_r + \alpha_p)^3)$	$\mathcal{O}((2N_r + \alpha_p)^3 + 2N_t(2N_r + \alpha_p)^2 + 2N_t(2N_r + \alpha_p))$
SINR Sequential Search	$\mathcal{O}(\sum_{i=1}^{\alpha_p} (2N_r + i - 1)^3)$	$\mathcal{O}((2N_r + \alpha_p)^3 + 2N_t(2N_r + \alpha_p)^2 + 2N_t(2N_r + \alpha_p))$
Random Selection	-	$\mathcal{O}((2N_r + \alpha_p)^3 + 2N_t(2N_r + \alpha_p)^2 + 2N_t(2N_r + \alpha_p))$

and hardware costs¹ in terms of additional comparators are approximately calculated in Table II. The values presented for the computational cost (arithmetic operations) are calculated using Table I and considering the following parameters: $N_r = 10$, $N_t = 2$, $\alpha_f = 190$ and $\alpha_p = 20$.

¹The costs do not include the crossbar switch required to select which antennas will be used as inputs on each comparator.

TABLE II: Computational and Hardware Costs

Approach	Computational Cost	Hardware Cost
No Network	$\mathcal{O}(9,68 \times 10^3)$	-
Full connection	$\mathcal{O}(9,44 \times 10^6)$	190
MMSE based Greedy Search	$\mathcal{O}(2,18 \times 10^8)$	20
SINR Sequential Search	$\mathcal{O}(2,24 \times 10^5)$	20
Random Selection	$\mathcal{O}(7,06 \times 10^4)$	20

B. Power consumption

Compared to the conventional multi-bit systems, the advantage of 1-bit ADCs or comparators is that they do not require automatic gain control (AGC). Table III shows the power consumption at the receiver as a function of the quantization bits, which is calculated similarly to [37], as

$$P_{1\text{-bit}} = P_{\text{LO}} + N_r(P_{\text{LNA}} + P_{\text{H}} + 2P_{\text{M}}) + 2N_r(\text{FOM} \times 2f_{\text{Nyquist}}) \quad (60)$$

$$P_{\text{Traditional}} = P_{\text{LO}} + N_r(P_{\text{LNA}} + P_{\text{H}} + 2P_{\text{M}}) + 2N_r(P_{\text{AGC}} + \text{FOM} \times 2^q f_{\text{Nyquist}}) \quad (61)$$

$$P_{\text{CN}} = P_{\text{LO}} + N_r(P_{\text{LNA}} + P_{\text{H}} + 2P_{\text{M}}) + (2N_r + \alpha)(\text{FOM} \times 2f_{\text{Nyquist}}), \quad (62)$$

where P_{LO} , P_{LNA} , P_{H} , P_{M} and P_{AGC} denote the power consumption in the local oscillator (LO), low noise amplifier (LNA), $\frac{\pi}{2}$ hybrid and LO buffer, mixer and AGC, respectively. The parameter q refers to the number of quantization bits and α is the number of comparators in the comparator network. The power consumption of different hardware components in the receiver for mmWave communications [37] is given as $P_{\text{LO}} = 22.5$ mW, $P_{\text{LNA}} = 5.4$ mW, $P_{\text{H}} = 3$ mW, $P_{\text{AGC}} = 2$ mW, $P_{\text{M}} = 0.3$ mW, $P_{\text{AGC}} = 2$ mW, $f_{\text{Nyquist}} = 2.5$ GHz and $\text{FOM} = 15$ fJ. From the results, it can be seen that the proposed network consumes much less power than common multi-bit systems.

TABLE III: Receiver power consumption among comparator network and multi-bit systems, where $N_r = 16$ and $\alpha = 2N_r$.

	1-bit	CN	Multi-bit systems								
			2-bit	3-bit	4-bit	5-bit	6-bit	7-bit	8-bit	9-bit	10-bit
Power consumption (mW)	168.9	171.3	235.3	240.1	249.7	268.9	307.3	384.1	537.7	844.9	1459.3

VII. SUM RATE

In this subsection, we analyze the sum-rate of the multiuser MIMO system with the proposed comparator networks. In particular, we consider a data transmission model that relies on the channel estimates from the LRA-MMSE channel estimator together with its error statistics and linear filtering for the detection process.

A. Data Transmission with Linear Receiver

It is considered that in the data transmission stage the N_t users simultaneously transmit their data symbols represented by the vector \mathbf{x}_R to the BS, which is a stacked vector with real and imaginary parts, as introduced in (3). In the present study, real and imaginary parts represent independent data symbols. After processing by the comparators and ADCs, the signal reads as

$$\begin{aligned} \mathbf{z}_{Q_d} &= \mathcal{Q}(\mathbf{z}_{R_d}) = \mathcal{Q}(\mathbf{B}\mathbf{y}_{R_d}) = \mathcal{Q}(\mathbf{B}\mathbf{H}_R\mathbf{x}_R + \mathbf{B}\mathbf{n}_{R_d}) \\ &= \mathbf{A}_{R_d}\mathbf{B}\mathbf{H}_R\mathbf{x}_R + \mathbf{A}_{R_d}\mathbf{B}\mathbf{n}_{R_d} + \mathbf{n}_{R_{q,d}}, \end{aligned} \quad (63)$$

where the same definitions from Section III apply. Note that the subscript d is associated with data transmission stage. Then, the LRA-LMMSE channel estimate (23) is used to compute a linear receiver which provides an estimate of the data symbols transmitted from the N_t users. In this context, the quantized signal is separated into $2N_t$ streams by multiplying the signal with the receiver filter matrix. An example for the receiver matrix is given by (37), which in this case is computed based on the estimated channel. Therefore, we obtain

$$\begin{aligned} \hat{\mathbf{x}}_R &= \mathbf{G}_R\mathbf{z}_{Q_d} = \mathbf{G}_R(\mathbf{A}_{R_d}\mathbf{B}\mathbf{H}_R\mathbf{x}_R + \mathbf{A}_{R_d}\mathbf{B}\mathbf{n}_{R_d} + \mathbf{n}_{R_{q,d}}) \\ &= \mathbf{G}_R\mathbf{A}_{R_d}\mathbf{B}(\hat{\mathbf{H}}_R\mathbf{x}_R + \mathcal{E}_R\mathbf{x}_R) + \mathbf{G}_R\mathbf{A}_{R_d}\mathbf{B}\mathbf{n}_{R_d} + \mathbf{G}_R\mathbf{n}_{R_{q,d}}, \end{aligned} \quad (64)$$

where $\hat{\mathbf{H}}_R$ is the estimated channel matrix described by (43) and $\mathcal{E}_R = \mathbf{H}_R - \hat{\mathbf{H}}_R$ is the channel estimation error matrix. In the sum rate analysis it is considered that each user corresponds to two real-valued channels. Then, the k th element represents an estimate of the signal of the k th real-valued channel, similarly as in [19], with $k \in [1, 2N_t]$, which reads as

$$\begin{aligned} \hat{x}_{R_k} &= \underbrace{\mathbf{g}_{R_k}^T \mathbf{A}_{R_d} \mathbf{B} \hat{\mathbf{h}}_{R_k} \mathbf{x}_{R_k}}_{\text{desired signal}} + \underbrace{\mathbf{g}_{R_k}^T \sum_{i \neq k}^K \mathbf{A}_{R_d} \mathbf{B} \hat{\mathbf{h}}_{R_i} \mathbf{x}_{R_i}}_{\text{interference}} + \underbrace{\mathbf{g}_{R_k}^T \sum_{i=1}^K \mathbf{A}_{R_d} \mathbf{B} \mathcal{E}_{R_i} \mathbf{x}_{R_i}}_{\text{channel estimation error}} \\ &\quad + \underbrace{\mathbf{g}_{R_k}^T \mathbf{A}_{R_d} \mathbf{B} \mathbf{n}_{R_d}}_{\text{AWGN noise}} + \underbrace{\mathbf{g}_{R_k}^T \mathbf{n}_{R_{q,d}}}_{\text{quant. noise}} \end{aligned} \quad (65)$$

where $\mathbf{g}_{R_k}^T$ is the k th row of \mathbf{G}_R and $\hat{\mathbf{h}}_{R_k}$ is the k th column of $\hat{\mathbf{H}}_R$. Moreover, $\boldsymbol{\varepsilon}_{R_i}$ is the i th column of the matrix $\boldsymbol{\mathcal{E}}_R$.

B. Sum Rate Lower Bound

Since the Gaussian noise case corresponds to the worst case scenario, we can find a lower bound for the achievable rate by interpreting the quantization noise as Gaussian [34]. The equivalent noise covariance matrix reads as

$$\mathbf{C}_{\mathbf{z}_{R_{q,d}}} = \mathbf{C}_{\mathbf{z}_{Q_d}} - \mathbf{A}_{R_d} \mathbf{C}_{\mathbf{z}_{R_d}} \mathbf{A}_{R_d}^T, \quad (66)$$

where $\mathbf{C}_{\mathbf{z}_{Q_d}} = E[\mathbf{z}_{Q_d} \mathbf{z}_{Q_d}^T]$ is the auto-correlation matrix of the quantized data signal, like in (21), and $\mathbf{C}_{\mathbf{z}_{R_d}} = E[\mathbf{z}_{R_d} \mathbf{z}_{R_d}^T] = \frac{1}{2} \sigma_x^2 \mathbf{B} \mathbf{H}_R \mathbf{H}_R^T \mathbf{B}^T + \frac{1}{2} \sigma_n^2 \mathbf{B} \mathbf{B}^T$ is the auto-correlation matrix of the received data signal, as calculated in (41). With this and by considering Gaussian signaling, the ergodic achievable rate per real-valued channel is lower bounded by

$$I_{R_k} = E \left[\frac{1}{2} \log_2 \left(1 + \frac{\sigma_x^2 |\mathbf{d}_{R_k} \hat{\mathbf{h}}_{R_k}|^2}{\sigma_x^2 \sum_{i \neq k} |\mathbf{d}_{R_k} \hat{\mathbf{h}}_{R_i}|^2 + \sigma_x^2 \sum_{i=1}^K |\mathbf{d}_{R_k} \boldsymbol{\varepsilon}_{R_i}|^2 + \sigma_n^2 \|\mathbf{d}_{R_k}\|_2^2 + 2 \mathbf{g}_{R_k}^T \mathbf{C}_{\mathbf{z}_{R_{q,d}}} \mathbf{g}_{R_k}} \right) \right] \text{ [bpcu]}, \quad (67)$$

where $\mathbf{d}_{R_k} = \mathbf{g}_{R_k}^T \mathbf{A}_{R_d} \mathbf{B}$ and the expectation operator is taken with respect to channel realizations and channel estimates. According to [34], this method provides an accurate lower bound especially for the low SNR regime. Finally, the sum rate is lower-bounded by $\sum_{k=1}^K I_{R_k}$, which can be computed via Monte Carlo Simulations. A detailed description is shown in Appendix B.

VIII. NUMERICAL RESULTS

In this section, an uplink single-cell 1-bit MIMO system is considered. The average receive SNR per user per antenna is defined as $10 \log \left(\frac{\sigma_x^2}{N_t N_r \sigma_n^2} E\{\text{trace}\{\mathbf{H} \mathbf{H}^H\}\} \right)$ and the modulation scheme is QPSK. For the lower bound on the sum rate, Gaussian signaling is considered. The considered channel matrix has in general the form $\mathbf{H} = \mathbf{H}_w \text{diag}[\sqrt{\beta_1} \dots \sqrt{\beta_{N_t}}]$, where β_i represents large scale coefficients and $[\mathbf{H}_w]_{n,m}$ are i.i.d. complex Gaussian random variables.

A. Perfect CSI

1) Proof of Concept: More Antennas versus the Comparator Network:

In this subsection, systems with $N_t = 3$ and different numbers of receive antennas N_r are considered. In this experiment Rayleigh fading is considered which implies $\beta_i = 1$. While performing the signal detection, the LRA-LMMSE detector from Subsection IV-A is applied in

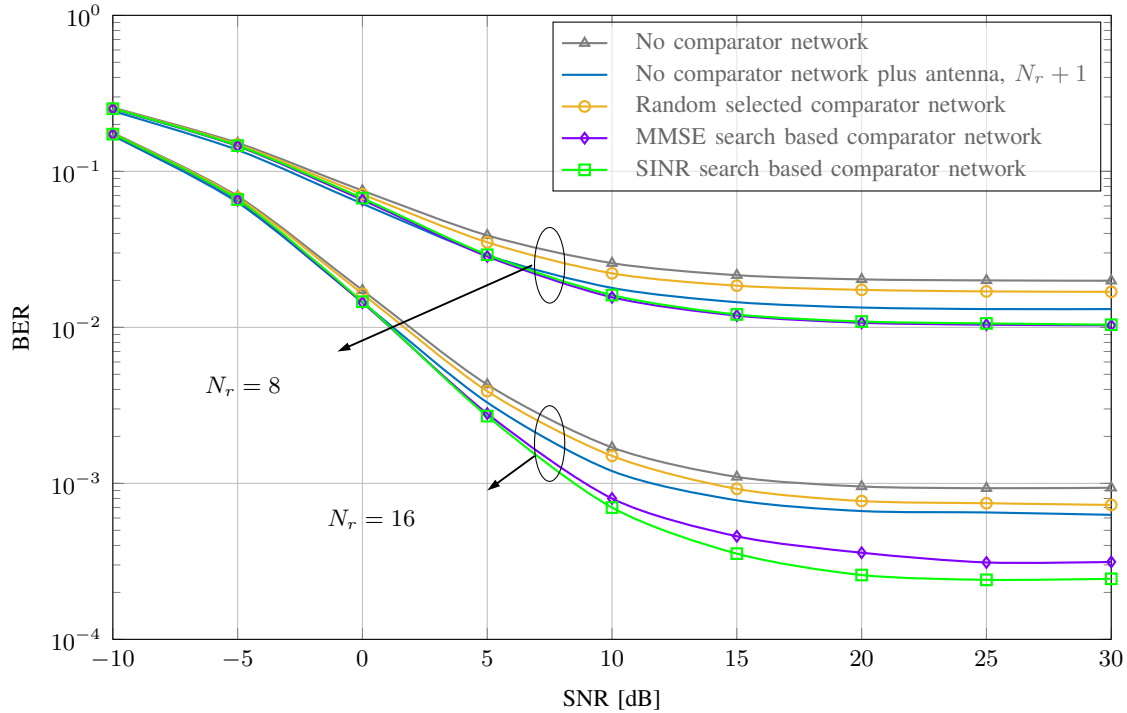


Fig. 3: Comparison between extra physical channels and comparator network with $\alpha_p = 2$.

the system. The BER performance is simulated based on 4000 random channel realizations and 1000 noise realizations. In order to verify the advantage of the additional comparator network, the performance of systems with partially connected networks are compared to systems with additional receive antennas. The configuration schemes with N_r and $N_r + 1$ receive antennas are considered, which means the addition of a single antenna element. Since each extra antenna would correspond to two comparators, to make a fair comparison, the total number of extra comparators utilized by the partially connected networks is always $\alpha_p = 2$ in the presented simulations. As we can see from Fig. 3, the random selected comparator network only has a benefit in comparison to the system without comparator network in a scenario with the same number of antennas. However, the optimized comparator networks, MMSE based Greedy Search and SINR search based networks, outperform the larger arrays in BER in the high SNR regime. Note that an increasing number of receive antennas improves the conditions for comparator network optimization in terms of possible input combinations, which can yield a performance gain in BER. Finally, this experiment illustrates for different array sizes N_r , that extra virtual channels can be more beneficial than an extra physical channel.

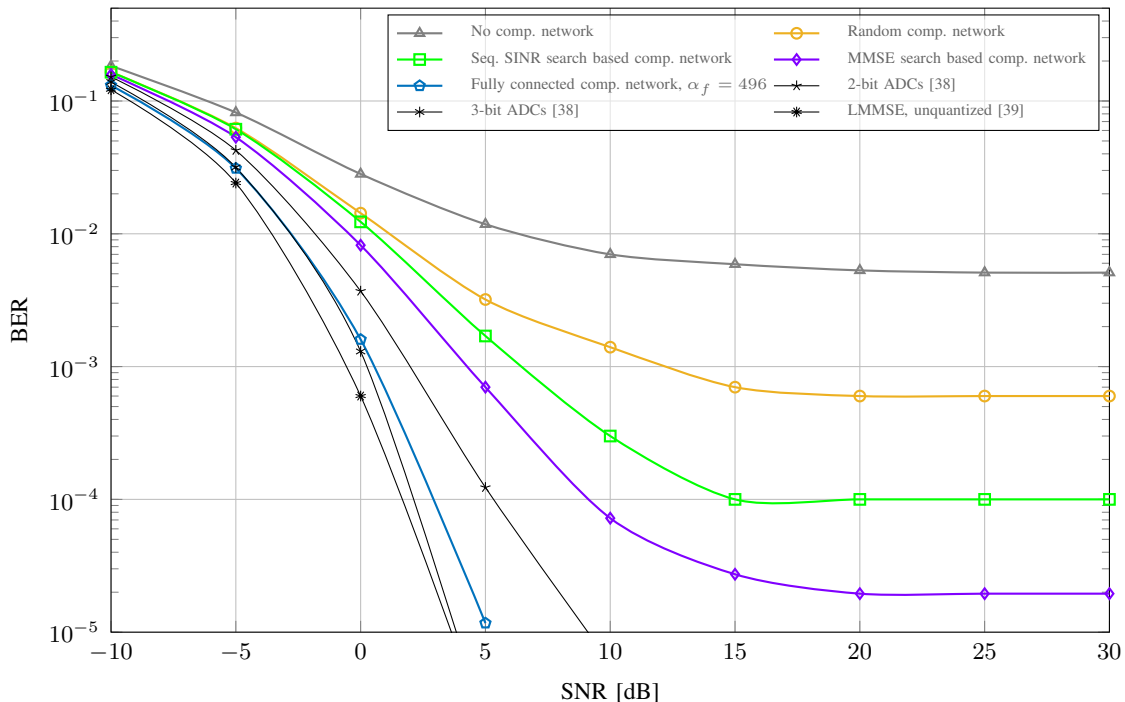


Fig. 4: BER performance with ($\alpha_p = 2N_r$) and without comparator network with $N_t = 4$, $N_r = 16$.

2) Proposed LRA-LMMSE Detector:

In this subsection, numerical results on signal detection are shown. The BER performance for the Rayleigh fading channel of fully and partially connected networks with dimensions $N_r = 16$ and $N_t = 4$ are shown in Fig. 4, where partially connected refers to comparator networks with $\alpha_p = 2N_r$ comparators. The case of fully connected networks refers to comparator networks with, in this case, $\alpha_f = \binom{2N_r}{2}$ comparators. As additional reference methods 2-bit and 3-bit detection methods [38] are considered which rely on message passing. For illustration of the high resolution case we consider linear MMSE detection [39].² Simulation results show that the system with fully connected network achieves the best BER performance with the cost of a large number of comparators and high computational complexity. In the partially connected networks, the MMSE based Greedy Search outperforms the random selection approach especially at high SNR, where the error floor is eliminated. A surprising observation is that the Greedy Search approach has almost the same BER performance as the fully connected method but with much

²For the 2-bit ADCs we consider thresholds $(0, \pm 1)$ and for the 3-bit ADCs we consider thresholds $(0, \pm 0.5, \pm 1, \pm 1.75)$ in conjunction with channel normalization $\text{tr}(\mathbf{H}\mathbf{H}^H) = N_r N_t$ and $\sigma_x^2 = 1$.

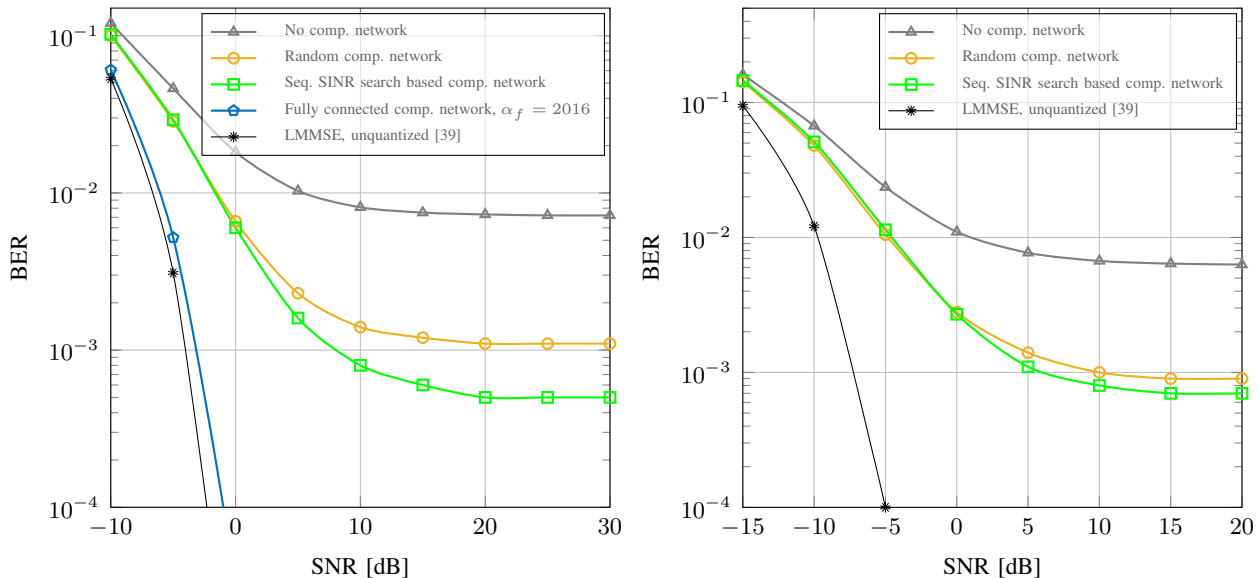


Fig. 5: BER comparison with large scale MIMO system ($\alpha_p = 2N_r$), $N_r = 32$, $N_t = 8$ (left); $N_r = 64$, $N_t = 15$ (right).

less comparators. This shows great advantages of the greedy search based partially connected network. However, also the approach with the comparator network using random selected inputs is beneficial in terms of BER. While making comparison with the approach without additional comparator network, it can be seen that by adding extra 32 comparators the performance gain is significant and the error floor goes down largely.

However, it should be mentioned that although the greedy search approach yields comparable good BER performance with less required comparators, its computational complexity is the highest among all the approaches. A reasonable performance-complexity trade-off can be achieved by considering the proposed Sequential SINR based Search.

Fig. 5 shows results with larger dimensions where only approaches with moderate computational complexity are considered. Simulation results show that the error floor can be significantly reduced by taking into account a comparator network for detection.

In addition, a channel with large scale fading is considered in Fig. 6. In this context, the log-distance path loss model [40, p. 104] is considered which implies that β_i is proportional to $\left(\frac{d_0}{d_i}\right)^{n_{PL}}$, where d_0 is a reference distance and d_i is the user's distance to the BS and n_{PL} is the path loss exponent chosen equal to 3. The users are uniformly distributed on a disc with 500m radius with the BS in the center. It can be observed that receivers with optimized comparator network show a relatively good BER performance in the presence of large scale fading.

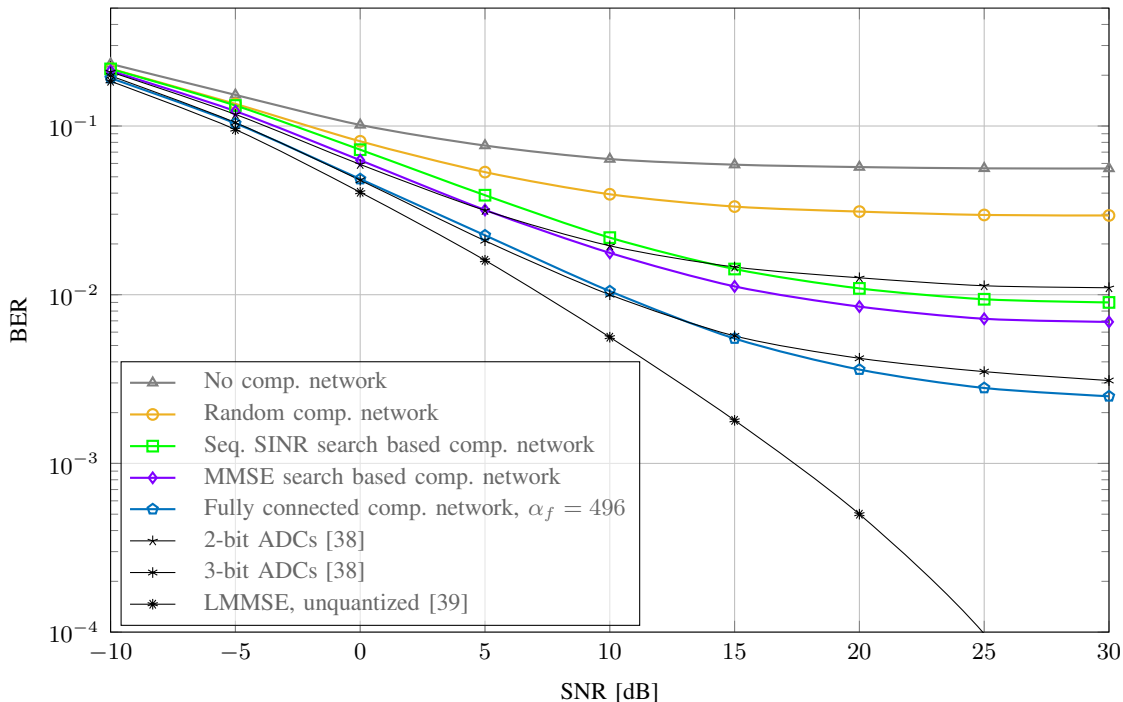


Fig. 6: BER comparison with large scale fading ($\alpha_p = 2N_r$), $N_r = 16$, $N_t = 4$.

3) Sum Rate Analysis:

In this subsection, $N_t = 3$ users and different numbers of base station antennas are considered. The sum rates are obtained by averaging over 2000 different Rayleigh fading channels and 2000 noise realizations per channel. The comparison between the lower bound of the ergodic sum rate with and without the comparator network under perfect CSI is presented in Fig. 7, where the system that utilizes the additional comparator networks shows a significant benefit. In this experiment, the randomly connected network has $\alpha_p = 2N_r$ comparators, while the fully connected have $\alpha_f = \binom{2N_r}{2}$ comparators. We can see that the system with fully connected network achieves the best sum rate performance, followed by the system with random selected inputs. Receivers with a comparator network of size $\alpha_p = 2N_r$ are comparable with receivers with twice the number of antennas. For random comparator networks, the performance of the receivers with twice the number of antennas serves as an upper bound, as verified in Fig. 7.

B. Imperfect CSI

In this subsection, the pilot sequences are column-wise orthogonal with length $\tau = N_t$, i.e., $\Phi^T \Phi = \tau \sigma_x^2 \mathbf{I}_{N_t}$. Two types of network design are considered: random selected and fully

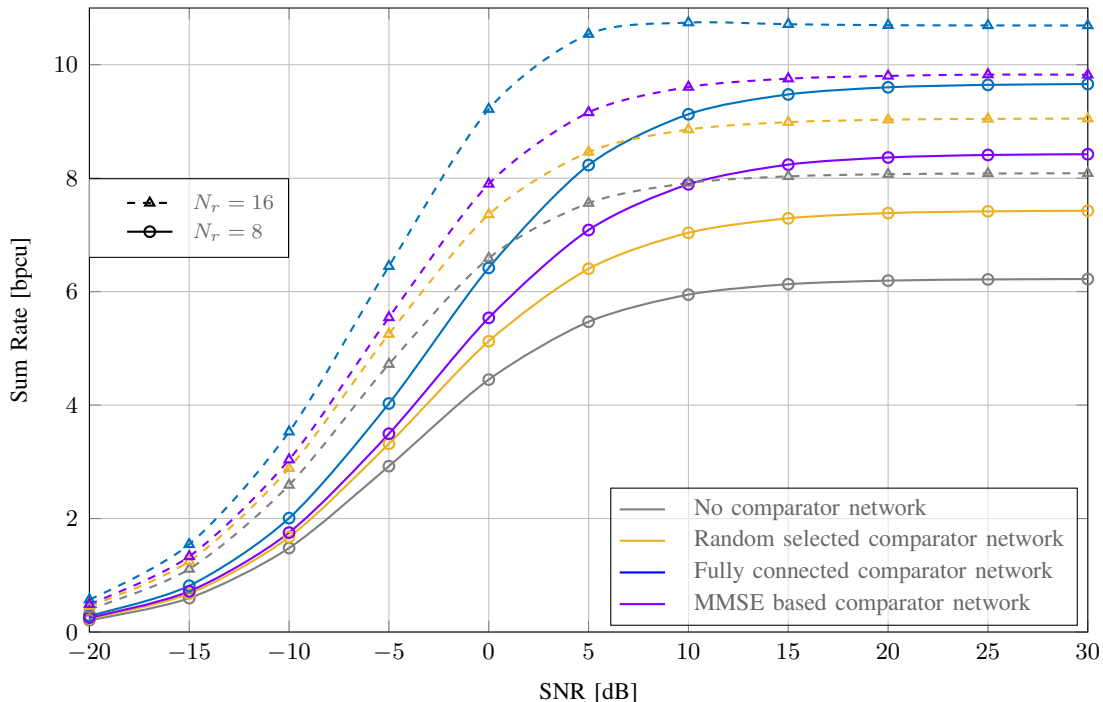


Fig. 7: Sum Rate comparisons with and without comparator network, under perfect CSI.

connected networks. The former randomly selects α_p out of α_f ($\alpha_p \ll \alpha_f$) comparators. The fully connected networks refers to comparator networks where all possible combinations are considered, meaning $\alpha_f = \binom{2N_r}{2}$ comparators. In all experiments Rayleigh fading channels are considered.

1) Channel Estimation:

In this subsection, an uplink single-cell 1-bit MIMO system with comparator network, $N_r = 16$ is considered. The presented performance plots are obtained by taking the average over 4000 different Rayleigh fading channel realizations and 100 noise realizations per channel. Moreover, the lines labeled as “Analytical Result” are obtained with (28) while the marks labeled as “Numerical Result” are obtained with the MSE of the simulated channel estimator in (23). In the experiment, the partially connected networks have $\alpha_p = 2N_r = 32$ comparators, while the fully connected have $\alpha_f = \binom{2N_r}{2} = 496$ comparators. As a performance reference a channel estimator with 2-bit quantization and 3-bit quantization is considered [38], where the thresholds are those used before in the detection part. For illustration of the high-resolution case we consider linear MMSE channel estimation [41].

The MSE comparison between the LRA-LMMSE channel estimators with fully and partially

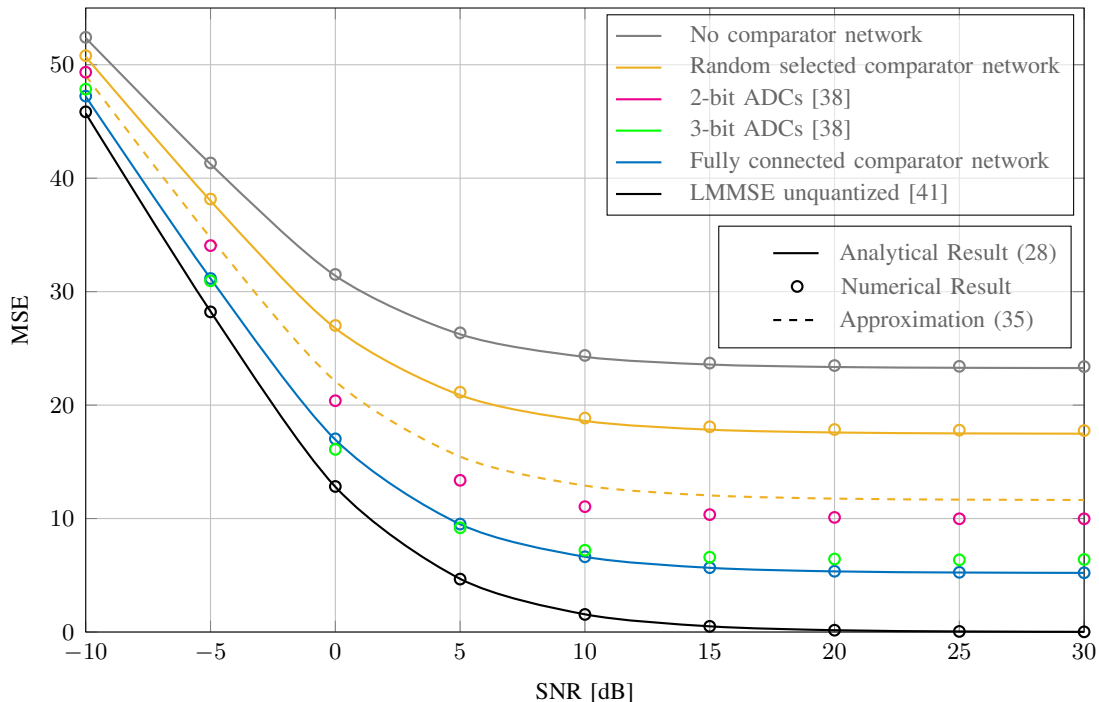


Fig. 8: MSE comparisons of LRA-LMMSE channel estimators with and without comparator network in 4×16 MIMO systems.

connected comparator networks are shown in Fig. 8. The numerical and analytical results are aligned, which confirms the accuracy of the proposed model. As expected, the system with the fully connected method achieves the best MSE performance. However, it can be seen that the approach with the comparator network using random selected inputs is also beneficial in terms of MSE in comparison to the case without a comparator network.

2) Robust LRA-LMMSE Detector:

In this subsection, it is considered a system with $N_r = 16$. The BER performance plots are obtained by taking the average over 4000 different channels and 100 noise realizations per channel. In these experiments, the partially connected networks have $\alpha_p = 2N_r = 32$ comparators, while the fully connected have $\alpha_f = \binom{2N_r}{2} = 496$ comparators.

In this experiment the receiver has imperfect CSI due to the model described in Sec. IV-B. While the LRA-LMMSE detector relies only on the known part of the channel $\mathbf{h}_{R,1}$, the robust LRA-LMMSE detector also takes into account the corresponding CSI mismatch statistics $\mathbf{R}_{\mathbf{h}_{R,2}} = E[\mathbf{h}_{R,2}\mathbf{h}_{R,2}^T]$. For the experiment it is considered that $\mathbf{R}_{\mathbf{h}_{R,2}} = \mathbf{R}_{\mathbf{h}_R}$. The BER for the proposed robust LRA-LMMSE detector is simulated for a case with marginal CSI mismatch with $\lambda = 0.8$,

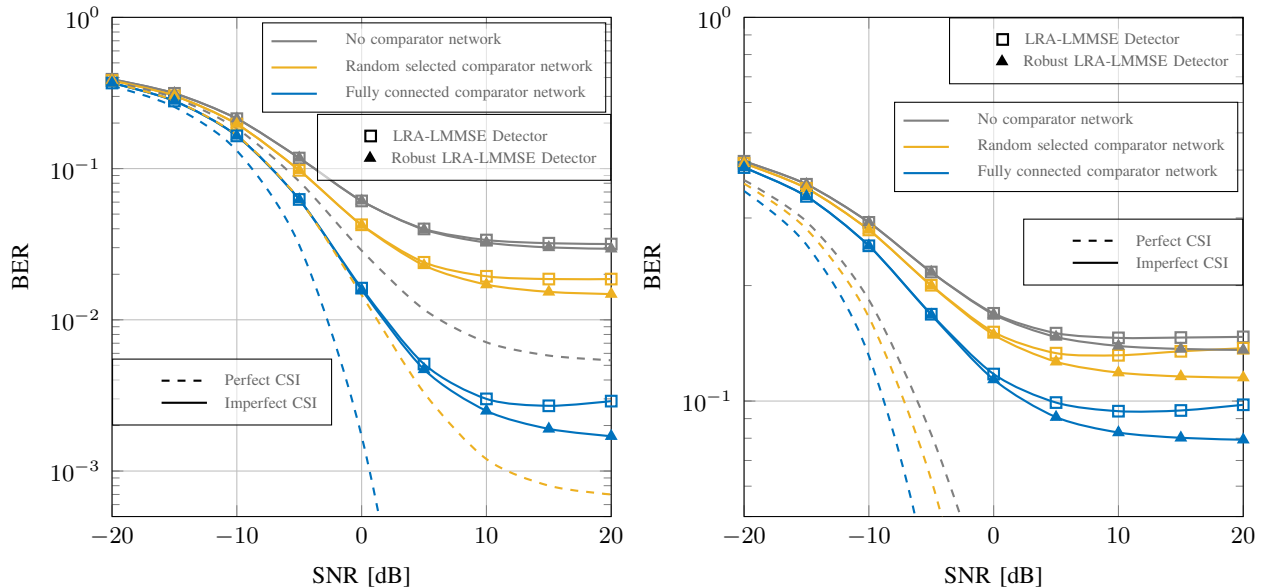


Fig. 9: Robust detectors with and without comparator network in 4×16 MIMO systems, $\lambda = 0.8$ (left) and $\lambda = 0.4$ (right)

shown on the left hand side of Fig. 9 and for a case with significant CSI mismatch with $\lambda = 0.4$, shown on the right hand side of Fig. 9. Simulation results show that the robust LRA-LMMSE detector yields a significant performance advantage in comparison to the non-robust detector. Moreover, we have noticed that for other CSI mismatch scenarios such as those described in Sec. IV-C the proposed robust detection also yields an improvement in BER.

3) Sum Rate Analysis:

In this subsection, it is considered a system with $N_t = 3$ and different values for N_r . The sum rate results are obtained by taking the average over 2000 different channels and 2000 noise realizations per channel. The sum rate versus SNR for the systems under imperfect CSI is shown in Fig. 10, which indicates a significant benefit for the system that utilizes the additional comparator networks. We can see that the system with fully connected network achieves the best sum rate performance, followed by the system with random selected inputs. Note that the increased sum rate is not only due to the comparator network aided receive processing but also due to a more accurate channel estimation.

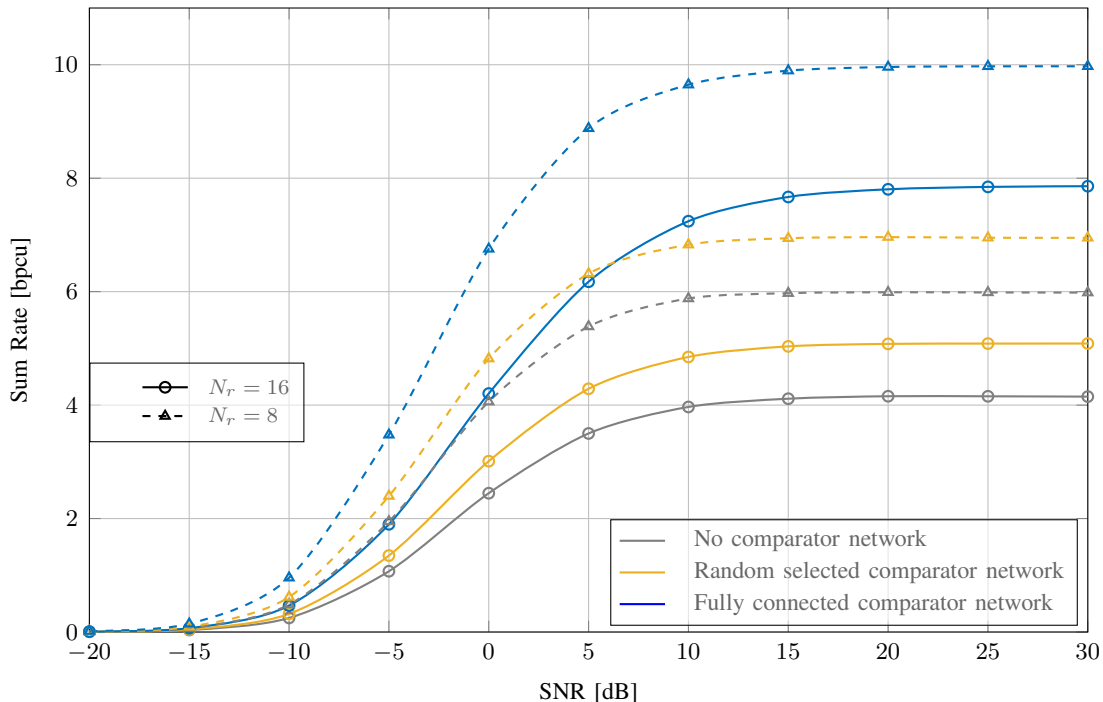


Fig. 10: Sum Rate comparisons of MIMO systems with and without comparator network, under imperfect CSI.

IX. CONCLUSIONS

This study proposes a novel MIMO receiver architecture with the use of 1-bit quantization ADCs. Different from conventional systems, the proposed MIMO receiver includes a comparator network with binary outputs which can compare signals from different antennas. The resulting extension can be interpreted as a number of additional virtual channels. This additional virtual channels contain additional information which aid the detection and channel estimation processes with only a slight increase in hardware cost and computational complexity. In this context, channel estimation, signal detection and sum rate schemes are developed for the proposed system.

Two types of comparator networks are proposed, fully and partially connected networks. Simulation results show that the proposed partially connected networks, especially the MMSE based greedy search approach and Sequential SINR based Search, require less comparators while introducing only small performance degradation compared with the fully connected networks.

Simulation results show that the proposed multiuser MIMO receiver architectures in conjunction with the proposed channel estimation and detection algorithms are superior to the conventional 1-bit quantization receiver methods in terms of BER and MSE. Moreover, numerical results show that adding virtual channels by using comparator networks can be better than adding

extra physical channels which corresponds to additional receive antennas in terms of BER. In this context, the proposed comparator networks are attractive for receivers with limited numbers of antennas due to physical space constraints. Furthermore, a robust LRA-LMMSE detector has been developed, which takes into account the mismatch statistics of imperfect CSI at the receiver. Simulation results indicate the advantage in terms of BER performance and MSE in comparison to the non-robust detector. Moreover, by relying on linear receive processing and considering the proposed channel estimate and the corresponding estimation error, it has been derived an expression for lower bounding the ergodic sum rate. Numerical results show that the corresponding sum rate increases significantly when adding a comparator network to the system.

APPENDIX

A. Derivation of the LRA-LMMSE Channel Estimator

Recalling the optimization problem from (20) and taking the partial derivative with respect to \mathbf{W}^T , we obtain

$$\frac{\partial E \left[\left\| \mathbf{h}_R - \mathbf{W} \mathbf{z}_{Q_p} \right\|_2^2 \right]}{\partial \mathbf{W}^T} = -E \left[\mathbf{h}_R \mathbf{z}_{Q_p}^T \right] + \mathbf{W} E \left[\mathbf{z}_{Q_p} \mathbf{z}_{Q_p}^T \right]. \quad (68)$$

Equating (68) to zero and inserting (12), the LRA-LMMSE filter is

$$\mathbf{W}_{R, \text{LRA-LMMSE}} = E \left[\mathbf{h}_R \mathbf{z}_{Q_p}^T \right] E \left[\mathbf{z}_{Q_p} \mathbf{z}_{Q_p}^T \right]^{-1} = \mathbf{R}_{\mathbf{h}_R} \hat{\Phi}_R^T \mathbf{C}_{\mathbf{z}_{Q_p}}^{-1}, \quad (69)$$

where it is considered that \mathbf{h}_R is uncorrelated with $\tilde{\mathbf{n}}_{R_p}$.

B. Derivation of the Ergodic Achievable Rate per Sub-Channel

First, let us recall the received signal of the index k , with $k \in [1, 2N_t]$, given by (65)

$$\begin{aligned} \hat{\mathbf{x}}_{R_k} = & \underbrace{\mathbf{g}_{R_k}^T \mathbf{A}_{R_d} \mathbf{B} \hat{\mathbf{h}}_{R_k} \mathbf{x}_{R_k}}_{\text{desired signal}} + \underbrace{\mathbf{g}_{R_k}^T \sum_{i \neq k}^K \mathbf{A}_{R_d} \mathbf{B} \hat{\mathbf{h}}_{R_i} \mathbf{x}_{R_i}}_{\text{interference}} + \underbrace{\mathbf{g}_{R_k}^T \sum_{i=1}^K \mathbf{A}_{R_d} \mathbf{B} \boldsymbol{\varepsilon}_{R_i} \mathbf{x}_{R_i}}_{\text{channel estimation error}} \\ & + \underbrace{\mathbf{g}_{R_k}^T \mathbf{A}_{R_d} \mathbf{B} \mathbf{n}_{R_d}}_{\text{AWGN noise}} + \underbrace{\mathbf{g}_{R_k}^T \mathbf{n}_{R_{q,d}}}_{\text{quant. noise}}, \end{aligned} \quad (70)$$

where $\mathbf{g}_{R_k}^T$ is the k th row of \mathbf{G}_R and $\hat{\mathbf{h}}_{R_k}$ is the k th column of $\hat{\mathbf{H}}_R$. Moreover, $\boldsymbol{\varepsilon}_{R_i}$ is the i th column of the matrix $\boldsymbol{\varepsilon}_R$. Assuming Gaussian signalling, the ergodic achievable rate per channel k , for the real-valued notation, is lower bounded by

$$I_{R_k} = E \left[\frac{1}{2} \log_2 (1 + \text{SINR}_k) \right] \text{ [bpcu]}, \quad (71)$$

where

$$\text{SINR}_k = \frac{E [|T_1|^2]}{\sum_{i \neq k}^K E [|T_{2,i}|^2] + \sum_{i=1}^K E [|T_{3,i}|^2] + E [|T_4|^2] + E [|T_5|^2]}. \quad (72)$$

Note that this SINR definition is associated with the receiver output which should not be confused with the SINR expression in (58) that refers to the individual virtual subchannels of the comparator networks. Then, the sum-rate is reads as $I_R = \sum_{k=1}^K I_{R_k}$. In (72), the term

$$T_1 = \mathbf{g}_{R_k}^T \mathbf{A}_{R_d} \mathbf{B} \hat{\mathbf{h}}_{R_k} \mathbf{x}_{R_k} \quad (73)$$

represents the desired signal, while the parameter

$$T_{2,i} = \mathbf{g}_{R_k}^T \mathbf{A}_{R_d} \mathbf{B} \hat{\mathbf{h}}_{R_i} \mathbf{x}_{R_i}, \text{ for } i \neq k, i = 1, \dots, K, \quad (74)$$

is the interference caused by user i to user k . The quantity

$$T_{3,i} = \mathbf{g}_{R_k}^T \mathbf{A}_{R_d} \mathbf{B} \boldsymbol{\epsilon}_{R_i} \mathbf{x}_{R_i}, \text{ for } i = k, i = 1, \dots, K, \quad (75)$$

refers to the channel estimation error, whilst

$$T_4 = \mathbf{g}_{R_k}^T \mathbf{A}_{R_d} \mathbf{B} \mathbf{n}_{R_d} \quad (76)$$

corresponds to the AWGN noise and

$$T_5 = \mathbf{g}_{R_k}^T \mathbf{n}_{R_{q,d}} \quad (77)$$

relates to the quantizer noise. By considering $E [\mathbf{x}_R \mathbf{x}_R^T] = \frac{\sigma_x^2}{2} \mathbf{I}_{2N_t}$ and $\mathbf{C}_{\mathbf{n}_{R_d}} = E [\mathbf{n}_{R_d} \mathbf{n}_{R_d}^T] = \frac{\sigma_n^2}{2} \mathbf{I}_{2N_r}$ and $\mathbf{d}_{R_k} = \mathbf{g}_{R_k}^T \mathbf{A}_{R_d} \mathbf{B}$ and $E [|T_5|^2] = \mathbf{g}_{R_k}^T \mathbf{C}_{\mathbf{n}_{R_{q,d}}} \mathbf{g}_{R_k}$ we get the following expression

$$\text{SINR}_k = \frac{\sigma_x^2 \left| \mathbf{d}_{R_k} \hat{\mathbf{h}}_{R_k} \right|^2}{\sigma_x^2 \sum_{i \neq k}^K \left| \mathbf{d}_{R_k} \hat{\mathbf{h}}_{R_i} \right|^2 + \sigma_x^2 \sum_{i=1}^K \left| \mathbf{d}_{R_k} \boldsymbol{\epsilon}_{R_i} \right|^2 + \sigma_n^2 \|\mathbf{d}_{R_k}\|_2^2 + 2\mathbf{g}_{R_k}^T \mathbf{C}_{\mathbf{n}_{R_{q,d}}} \mathbf{g}_{R_k}}. \quad (78)$$

Finally, inserting (78) into (71) yields the ergodic achievable rate per real-valued channel (67).

C. Sum Rate for Matched Filter Receiver

The corresponding matched filter for the k th substream for the system with comparator network can be expressed as $\mathbf{g}_{R_k}^T = \hat{\mathbf{h}}_{R_k}^T \mathbf{B}^T$. For description of the equivalent linear model the matrix $\mathbf{A}_{R_d} = \sqrt{\frac{2}{\pi}} \text{diag}(\mathbf{C}_{\mathbf{z}_{R_d}})^{-\frac{1}{2}}$ is given by

$$E[\mathbf{A}_{R_d}] = \sqrt{\frac{2}{\pi}} \text{diag} \left(E \left[\frac{\sigma_x^2}{2} \mathbf{B} \mathbf{H}_R \mathbf{H}_R^T \mathbf{B}^T + \frac{\sigma_n^2}{2} \mathbf{B} \mathbf{B}^T \right] \right)^{-\frac{1}{2}} \quad (79)$$

Considering a generic channel with $E[\mathbf{H}_R \mathbf{H}_R^T] = N_t \mathbf{I}$

$$E[\mathbf{A}_{R_d}] = \sqrt{\frac{2}{\pi} \frac{2}{N_t \sigma_x^2 + \sigma_n^2}} \mathbf{I}_{2N_r + \alpha}. \quad (80)$$

In the following, the prefactor in (80) is termed ζ . The received signal after filtering can be expressed alternatively as

$$\hat{\mathbf{x}}_{R_k} = E[\mathbf{g}_{R_k}^T \mathbf{A}_{R_d} \mathbf{B} \mathbf{h}_{R_k}] \mathbf{x}_{R_k} + n_{\text{eff},k}, \quad (81)$$

where $n_{\text{eff},k}$ represents some effective noise term. For the matched filtering approach under the mentioned assumptions it holds

$$E[\mathbf{g}_{R_k}^T \mathbf{A}_{R_d} \mathbf{B} \mathbf{h}_{R_k}] = \zeta E[\hat{\mathbf{h}}_{R_k}^T \mathbf{B}^T \hat{\mathbf{h}}_{R_k}]. \quad (82)$$

In the next step it is considered that $\mathbf{B}^T \mathbf{B}$ can be approximated by $(1 + \frac{\alpha}{2N_r}) \mathbf{I}$

$$E[\mathbf{g}_{R_k}^T \mathbf{A}_{R_d} \mathbf{B} \mathbf{h}_{R_k}] = \zeta \left(1 + \frac{\alpha}{2N_r}\right) \text{trace}[E[\hat{\mathbf{h}}_{R_k} \hat{\mathbf{h}}_{R_k}^T]]. \quad (83)$$

The correlation matrix of the channel estimate is given by

$$E[\hat{\mathbf{h}}_{R_k, \text{LRA-MMSE}} \hat{\mathbf{h}}_{R_k, \text{LRA-MMSE}}^T] = \frac{1}{2} \frac{N_t \sigma_x^2}{N_t \sigma_x^2 + \sigma_n^2} \left(1 - \frac{\pi - 2}{2(1 + \frac{\alpha}{2N_r}) + \pi - 2}\right) \mathbf{I}_{2N_r N_t}, \quad (84)$$

where we term the prefactor κ . With this, it follows

$$E[\mathbf{g}_{R_k}^T \mathbf{A}_{R_d} \mathbf{B} \mathbf{h}_{R_k}] = \zeta \left(1 + \frac{\alpha}{2N_r}\right) 2N_r \kappa. \quad (85)$$

The corresponding variance is given by

$$\text{Var}[\mathbf{g}_{R_k}^T \mathbf{A}_{R_d} \mathbf{B} \mathbf{h}_{R_k}] = E[\mathbf{g}_{R_k}^T \mathbf{A}_{R_d} \mathbf{B} \mathbf{h}_{R_k} \mathbf{h}_{R_k}^T \mathbf{B}^T \mathbf{A}_{R_d}^T \mathbf{g}_{R_k}] - E[\mathbf{g}_{R_k}^T \mathbf{A}_{R_d} \mathbf{B} \mathbf{h}_{R_k}]^2. \quad (86)$$

By considering $\mathbf{B}^T \mathbf{B} = (1 + \frac{\alpha}{2N_r}) \mathbf{I}$ the variance can be rewritten as

$$\text{Var}[\mathbf{g}_{R_k}^T \mathbf{A}_{R_d} \mathbf{B} \mathbf{h}_{R_k}] = \zeta^2 \left(1 + \frac{\alpha}{2N_r}\right)^2 \left(E[|\hat{\mathbf{h}}_{R_k}^T \mathbf{h}_{R_k}|^2] - E[\mathbf{g}_{R_k}^T \mathbf{A}_{R_d} \mathbf{B} \mathbf{h}_{R_k}]^2\right), \quad (87)$$

which can be expressed as

$$\begin{aligned} \text{Var}[\mathbf{g}_{R_k}^T \mathbf{A}_{R_d} \mathbf{B} \mathbf{h}_{R_k}] = & \\ \zeta^2 \left(1 + \frac{\alpha}{2N_r}\right)^2 \left(E[\hat{\mathbf{h}}_{R_k}^T \mathbf{h}_{R_k}]^2 + \text{Var}[\hat{\mathbf{h}}_{R_k}^T \mathbf{h}_{R_k}]\right) - E[\mathbf{g}_{R_k}^T \mathbf{A}_{R_d} \mathbf{B} \mathbf{h}_{R_k}]^2. & \end{aligned} \quad (88)$$

By considering $E[\hat{\mathbf{h}}_{R_k}^T \mathbf{h}_{R_k}] = E[\hat{\mathbf{h}}_{R_k}^T \hat{\mathbf{h}}_{R_k}]$ and (85) the variance reduces to

$$\text{Var}[\mathbf{g}_{R_k}^T \mathbf{A}_{R_d} \mathbf{B} \mathbf{h}_{R_k}] = \zeta^2 \left(1 + \frac{\alpha}{2N_r}\right)^2 \left(\text{Var}[\hat{\mathbf{h}}_{R_k}^T \hat{\mathbf{h}}_{R_k}] + \text{Var}[\hat{\mathbf{h}}_{R_k}^T \epsilon_{R_k}]\right) \quad (89)$$

Considering that the entries in $\hat{\mathbf{h}}_{R_k}$ are Gaussian distributed, it follows that $\|\hat{\mathbf{h}}_{R_k}\|^2$ is chi squared distributed with $2N_r$ degrees of freedom and $E[\|\hat{\mathbf{h}}_{R_k}\|^2] = 2N_r\kappa$ and $\text{Var}[\|\hat{\mathbf{h}}_{R_k}\|^2] = 4N_r\kappa^2$. Considering that the entries in ϵ_{R_k} are uncorrelated with the channel estimate and Gaussian distributed, the variance is given by

$$\text{Var}[\mathbf{g}_{R_k}^T \mathbf{A}_{R_d} \mathbf{B} \mathbf{h}_{R_k}] = \zeta^2 \left(1 + \frac{\alpha}{2N_r}\right)^2 (4N_r\kappa^2 + N_r\kappa(1 - 2\kappa)) \quad (90)$$

This finally yields

$$\text{Var}[\mathbf{g}_{R_k}^T \mathbf{A}_{R_d} \mathbf{B} \mathbf{h}_{R_k}] = \zeta^2 \left(1 + \frac{\alpha}{2N_r}\right)^2 N_r\kappa(2\kappa + 1). \quad (91)$$

The interference variance from the i th signal stream can be expressed as

$$E[|\mathbf{g}_{R_k}^T \mathbf{A}_{R_d} \mathbf{B} \mathbf{h}_{R_i} \mathbf{x}_{R_i}|^2] = \frac{\sigma_x^2}{2} \zeta^2 E[|\hat{\mathbf{h}}_{R_k}^T \mathbf{B}^T \mathbf{B} \mathbf{h}_{R_i}|^2]. \quad (92)$$

Considering that $\hat{\mathbf{h}}_{R_k}$ and \mathbf{h}_{R_i} are independent yields

$$E[|\mathbf{g}_{R_k}^T \mathbf{A}_{R_d} \mathbf{B} \mathbf{h}_{R_i} \mathbf{x}_{R_i}|^2] = \frac{\sigma_x^2}{4} \zeta^2 E[|\hat{\mathbf{h}}_{R_k}^T \mathbf{B}^T \mathbf{B}|^2]. \quad (93)$$

By assuming that the entries in \mathbf{B}' are binary distributed independent variables, the following approximation holds $E[\mathbf{B}^T \mathbf{B} \mathbf{B}^T \mathbf{B}] = E[\mathbf{B}^T \mathbf{B}]^2 + \text{Cov}[\mathbf{B}^T \mathbf{B}] \approx (1 + \frac{\alpha}{2N_r})^2 \mathbf{I} + \frac{\alpha}{4N_r^2} (N_r - 1) \mathbf{I} = \delta_B \mathbf{I}$. With this, the interference variance reads as

$$E[|\mathbf{g}_{R_k}^T \mathbf{A}_{R_d} \mathbf{B} \mathbf{h}_{R_i} \mathbf{x}_{R_i}|^2] = \frac{\sigma_x^2}{2} \zeta^2 \delta_B N_r \kappa. \quad (94)$$

The correlation matrix of the quantization noise is described by

$$\mathbf{C}_{\text{nr}_{q,d}} = \frac{\pi - 2}{\pi} \left(\frac{2}{\pi - 2} \mathbf{B} \mathbf{B}^T + \mathbf{I} \right) - \zeta^2 \frac{N_t \sigma_x^2 + \sigma_n^2}{2} \mathbf{B} \mathbf{B}^T. \quad (95)$$

This can be expressed as

$$\mathbf{C}_{\text{nr}_{q,d}} = \frac{\pi - 2}{\pi} \mathbf{I} + \left(\frac{2}{\pi} - \zeta^2 \frac{N_t \sigma_x^2 + \sigma_n^2}{2} \right) \mathbf{B} \mathbf{B}^T. \quad (96)$$

The quantization noise variance is determined by

$$E[\mathbf{g}_{R_k}^T \mathbf{C}_{\text{nr}_{q,d}} \mathbf{g}_{R_k}] = \frac{\pi - 2}{\pi} E[\mathbf{g}_{R_k}^T \mathbf{g}_{R_k}] + \left(\frac{2}{\pi} - \zeta^2 \frac{N_t \sigma_x^2 + \sigma_n^2}{2} \right) E[\mathbf{g}_{R_k}^T \mathbf{B} \mathbf{B}^T \mathbf{g}_{R_k}]. \quad (97)$$

This can be expressed as

$$E[\mathbf{g}_{R_k}^T \mathbf{C}_{\text{nr}_{q,d}} \mathbf{g}_{R_k}] = \frac{\pi - 2}{\pi} \left(1 + \frac{\alpha}{2N_r}\right) 2N_r\kappa + \delta_B \left(\frac{2}{\pi} - \zeta^2 \frac{N_t \sigma_x^2 + \sigma_n^2}{2} \right) 2N_r\kappa. \quad (98)$$

The variance of the thermal noise is given by

$$E[\mathbf{g}_{R_k}^T \mathbf{A}_{R_d} \mathbf{B} \mathbf{C}_{\text{nr}_d} \mathbf{B}^T \mathbf{A}_{R_d}^T \mathbf{g}_{R_k}] = \frac{\sigma_n^2}{2} \zeta^2 \delta_B 2N_r\kappa. \quad (99)$$

The resulting rate per real valued substream is given by

$$I_{R_k} = \frac{1}{2} \log_2 \left(1 + \frac{\frac{\sigma_x^2}{2} \zeta^2 \left(1 + \frac{\alpha}{2N_r}\right)^2 4N_r^2 \kappa^2}{\frac{\sigma_x^2}{2} \zeta^2 \delta_B N_r \kappa (K-1) + \frac{\sigma_x^2}{2} \zeta^2 \left(1 + \frac{\alpha}{2N_r}\right)^2 N_r \kappa (2\kappa+1) + \frac{\sigma_n^2}{2} \zeta^2 \delta_B 2N_r \kappa + \frac{\pi-2}{\pi} \left(1 + \frac{\alpha}{2N_r}\right) 2N_r \kappa + \delta_B \left(\frac{2}{\pi} - \zeta^2 \frac{N_t \sigma_n^2 + \sigma_n^2}{2}\right) 2N_r \kappa} \right).$$

This can be written more compact as

$$I_{R_k} = \frac{1}{2} \log_2 \left(1 + \frac{\sigma_x^2 \left(1 + \frac{\alpha}{2N_r}\right)^2 2N_r \kappa}{\frac{\sigma_x^2}{2} \delta_B (K-1) + \frac{\sigma_x^2}{2} \left(1 + \frac{\alpha}{2N_r}\right)^2 (2\kappa+1) + \sigma_n^2 \delta_B + 2 \frac{\pi-2}{\pi} \zeta^{-2} \left(1 + \frac{\alpha}{2N_r}\right) + 2\zeta^{-2} \delta_B \left(\frac{2}{\pi} - \zeta^2 \frac{N_t \sigma_n^2 + \sigma_n^2}{2}\right)} \right) \text{ [bpcu]}. \quad (100)$$

For the case of perfect CSI it holds $\kappa = \frac{1}{2}$ and the variance term is equal to zero, which yields

$$I_{R_k} = \frac{1}{2} \log_2 \left(1 + \frac{\sigma_x^2 \left(1 + \frac{\alpha}{2N_r}\right)^2 N_r}{\frac{\sigma_x^2}{2} \delta_B (K-1) + \sigma_n^2 \delta_B + 2 \frac{\pi-2}{\pi} \zeta^{-2} \left(1 + \frac{\alpha}{2N_r}\right) + 2\zeta^{-2} \delta_B \left(\frac{2}{\pi} - \zeta^2 \frac{N_t \sigma_n^2 + \sigma_n^2}{2}\right)} \right) \text{ [bpcu]}. \quad (101)$$

REFERENCES

- [1] A. B. L. B. Fernandes, Z. Shao, L. T. N. Landau, and R. C. de Lamare, "Comparator Network Aided Detection for MIMO Receivers with 1-Bit Quantization," in *Proc. 54th Asilomar Conf. Signals, Systems, and Computers*, 2020, pp. 384–387.
- [2] A. B. L. B. Fernandes and L. T. N. Landau, "Comparator Network Aided Channel Estimation and Achievable Rates for MIMO Receivers with 1-bit Quantization," in *Proc. IEEE Statistical Signal Processing Workshop*, Rio de Janeiro, RJ, Brazil, Jul 2021.
- [3] A. B. L. B. Fernandes, "On MIMO communications systems with 1-bit quantization and comparator networks at the receiver," Master's thesis, PUC-Rio, Rio de Janeiro, Brazil, Jul. 2021, www.maxwell.vrac.puc-rio.br/54121/54121.PDF.
- [4] E. G. Larsson, O. Edfors, F. Tufvesson, and T. L. Marzetta, "Massive MIMO for next generation wireless systems," *IEEE Commun. Mag.*, vol. 52, no. 2, pp. 186–195, Feb. 2014.
- [5] R. H. Walden, "Analog-to-digital converter survey and analysis," *IEEE J. Sel. Areas Commun.*, vol. 17, no. 4, pp. 539–550, Apr. 1999.
- [6] S. Jacobsson, G. Durisi, M. Coldrey, U. Gustavsson, and C. Studer, "Throughput analysis of massive MIMO uplink with low-resolution ADCs," *IEEE Trans. Wireless Commun.*, vol. 16, no. 6, pp. 4038–4051, Jun. 2017.
- [7] J. Zhang, L. Dai, X. Li, Y. Liu, and L. Hanzo, "On Low-Resolution ADCs in Practical 5G Millimeter-wave Massive MIMO Systems," *IEEE Commun. Mag.*, vol. 56, no. 7, pp. 205–211, Jul. 2018.
- [8] T. Liu, J. Tong, Q. Guo, J. Xi, Y. Yu, and Z. Xiao, "Energy Efficiency of Massive MIMO Systems With Low-Resolution ADCs and Successive Interference Cancellation," *IEEE Trans. Wireless Commun.*, vol. 18, no. 8, pp. 3987–4002, Aug. 2019.
- [9] L. T. N. Landau, M. Dörpinghaus, and G. P. Fettweis, "1-Bit Quantization and Oversampling at the Receiver: Communication Over Bandlimited Channels With Noise," *IEEE Commun. Lett.*, vol. 21, no. 5, pp. 1007–1010, 2017.
- [10] A. B. Üçüncü, E. Björnson, H. Johansson, A. O. Yılmaz, and E. G. Larsson, "Performance Analysis of Quantized Uplink Massive MIMO-OFDM With Oversampling Under Adjacent Channel Interference," *IEEE Trans. Commun.*, vol. 68, no. 2, pp. 871–886, 2020.
- [11] Z. Shao, L. T. N. Landau, and R. C. de Lamare, "Sliding Window Based Linear Signal Detection Using 1-Bit Quantization and Oversampling for Large-Scale Multiple-Antenna Systems," in *2018 IEEE Statistical Signal Processing Workshop (SSP)*, Freiburg, Germany, Jun. 2018, pp. 183–187.

- [12] Z. Shao, L. T. N. Landau, and R. C. de Lamare, "Channel Estimation for Large-Scale Multiple-Antenna Systems Using 1-Bit ADCs and Oversampling," *IEEE Access*, vol. 8, pp. 85 243–85 256, 2020.
- [13] Z. Shao, L. T. N. Landau, and R. C. de Lamare, "Dynamic oversampling for 1-bit adcs in large-scale multiple-antenna systems," *IEEE Trans. Commun.*, vol. 69, no. 5, pp. 3423–3435, 2021.
- [14] C. Risi, D. Persson, and E. G. Larsson, "Massive MIMO with 1-bit ADC," *arXiv preprint arXiv:1404.7736*, 2014.
- [15] Z. Shao, L. T. N. Landau, and R. C. de Lamare, "Adaptive RLS Channel Estimation and SIC for Large-Scale Antenna Systems with 1-Bit ADCs," in *WSA 2018; 22nd Int. ITG Workshop on Smart Antennas*, Bochum, Germany, Mar. 2018.
- [16] J. Mo, P. Schniter, and R. W. Heath, "Channel Estimation in Broadband Millimeter Wave MIMO Systems With Few-Bit ADCs," *IEEE Trans. Signal Process.*, vol. 66, no. 5, pp. 1141–1154, Mar. 2018.
- [17] Y. Xiong, N. Wei, and Z. Zhang, "A Low-Complexity Iterative GAMP-Based Detection for Massive MIMO with Low-Resolution ADCs," in *2017 IEEE Wireless Communications and Networking Conference (WCNC)*, 2017, pp. 1–6.
- [18] J. Choi, J. Mo, and R. W. Heath, "Near Maximum-Likelihood Detector and Channel Estimator for Uplink Multiuser Massive MIMO Systems with One-Bit ADCs," *IEEE Trans. Commun.*, vol. 64, no. 5, pp. 2005–2018, 2016.
- [19] Y. Li, C. Tao, G. Seco-Granados, A. Mezghani, A. L. Swindlehurst, and L. Liu, "Channel Estimation and Performance Analysis of One-Bit Massive MIMO Systems," *IEEE Trans. Signal Process.*, vol. 65, no. 15, pp. 4075–4089, Aug. 2017.
- [20] Q. Wan, J. Fang, H. Duan, Z. Chen, and H. Li, "Generalized bussgang LMMSE channel estimation for one-bit massive MIMO systems," *IEEE Trans. Wireless Commun.*, vol. 19, no. 6, pp. 4234–4246, 2020.
- [21] M. S. Stein, S. Bar, J. A. Nossek, and J. Tabrikian, "Performance Analysis for Channel Estimation With 1-Bit ADC and Unknown Quantization Threshold," *IEEE Trans. Signal Process.*, vol. 66, no. 10, pp. 2557–2571, May 2018.
- [22] I. Kim and J. Choi, "Channel estimation via gradient pursuit for mmWave massive MIMO systems with one-bit ADCs," *EURASIP Journal on Wireless Communications and Networking*, vol. 2019, no. 1, p. 289, 2019.
- [23] H. Kim and J. Choi, "Channel estimation for spatially/temporally correlated massive MIMO systems with one-bit ADCs," *EURASIP Journal on Wireless Communications and Networking*, vol. 2019, no. 1, p. 267, 2019.
- [24] C. Mollén, J. Choi, E. G. Larsson, and R. W. Heath, "Uplink Performance of Wideband Massive MIMO With One-Bit ADCs," *IEEE Transactions on Wireless Communications*, vol. 16, no. 1, pp. 87–100, 2017.
- [25] Z. Shao, R. C. de Lamare, and L. T. N. Landau, "Iterative Detection and Decoding for Large-Scale Multiple-Antenna Systems With 1-Bit ADCs," *IEEE Wireless Commun. Lett.*, vol. 7, no. 3, pp. 476–479, Jun. 2018.
- [26] Y. Jeon, N. Lee, S. Hong, and R. W. Heath, "One-Bit Sphere Decoding for Uplink Massive MIMO Systems With One-Bit ADCs," *IEEE Trans. Wireless Commun.*, vol. 17, no. 7, pp. 4509–4521, Jul. 2018.
- [27] H. Pirzadeh, G. Seco-Granados, S. Rao, and A. L. Swindlehurst, "Spectral Efficiency of One-Bit Sigma-Delta Massive MIMO," *IEEE Journal on Selected Areas in Communications*, vol. 38, no. 9, pp. 2215–2226, 2020.
- [28] S. Rao, A. L. Swindlehurst, and H. Pirzadeh, "Massive MIMO Channel Estimation with 1-Bit Spatial Sigma-delta ADCs," in *Proc. IEEE Int. Conf. Acoustics Speech Signal Process. (ICASSP)*, 2019, pp. 4484–4488.
- [29] T. E. B. Cunha, R. C. de Lamare, T. N. Ferreira, and T. Hälsig, "Joint Automatic Gain Control and MMSE Receiver Design for Quantized Multiuser MIMO Systems," in *Proc. Int. Symp. on Wireless Comm. Systems (ISWCS)*, Lisbon, Portugal, 2018.
- [30] O. B. Usman, H. Jedda, A. Mezghani, and J. A. Nossek, "MMSE precoder for massive MIMO using 1-bit quantization," in *2016 IEEE International Conference on Acoustics, Speech and Signal Processing (ICASSP)*, 2016, pp. 3381–3385.
- [31] L. T. N. Landau and R. C. de Lamare, "Branch-and-Bound Precoding for Multiuser MIMO Systems With 1-bit Quantization," *IEEE Wireless Communications Letters*, vol. 6, no. 6, pp. 770–773, 2017.
- [32] D. M. V. Melo, L. T. N. Landau, and R. C. de Lamare, "Zero-Crossing Precoding with MMSE Criterion for Channels with 1-Bit Quantization and Oversampling," in *WSA 2020; 24th International ITG Workshop on Smart Antennas*, 2020.

- [33] E. S. P. Lopes and L. T. N. Landau, "Optimal Precoding for Multiuser MIMO Systems With Phase Quantization and PSK Modulation via Branch-and-Bound," *IEEE Wireless Communications Letters*, vol. 9, no. 9, pp. 1393–1397, 2020.
- [34] A. Mezghani and J. Nosssek, "Capacity Lower Bound of MIMO Channels with Output Quantization and Correlated Noise," in *2012 International Symposium on Information Theory*, Cambridge, MA, Jul. 2012.
- [35] G. Jacovitti and A. Neri, "Estimation of the autocorrelation function of complex Gaussian stationary processes by amplitude clipped signals," *IEEE Trans. Inf. Theory*, vol. 40, no. 1, pp. 239–245, Jan. 1994.
- [36] J. J. Bussgang, "Crosscorrelation functions of amplitude-distorted Gaussian signals," *Res. Lab. Elec., MIT*, vol. Tech. Rep. 216, Mar. 1952.
- [37] K. Roth and J. A. Nosssek, "Achievable rate and energy efficiency of hybrid and digital beamforming receivers with low resolution ADC," *IEEE Journal on Selected Areas in Communications*, vol. 35, no. 9, pp. 2056–2068, 2017.
- [38] C.-K. Wen, C.-J. Wang, S. Jin, K.-K. Wong, and P. Ting, "Bayes-optimal joint channel-and-data estimation for massive MIMO with low-precision ADCs," *IEEE Trans. Signal Process.*, vol. 64, no. 10, pp. 2541–2556, 2016.
- [39] M. Joham, W. Utschick, and J. A. Nosssek, "Linear transmit processing in MIMO communications systems," *IEEE Trans. Signal Process.*, vol. 53, no. 8, pp. 2700–2712, Aug 2005.
- [40] T. S. Rappaport, *Wireless communications - principles and practice*. Prentice Hall, 1996.
- [41] M. Biguesh and A. Gershman, "Training-based MIMO channel estimation: a study of estimator tradeoffs and optimal training signals," *IEEE Trans. Signal Process.*, vol. 54, no. 3, pp. 884–893, 2006.